目　次

1. 主論文

Genetic divergence of Asian toads and phylogenetic relationships of anuran families (Amphibia, Anura) based on mitochondrial genome information, with special reference to divergence time estimation.

（ミトコンドリアゲノム情報に基づくアジア産ヒキガエル類の遺伝的分化と無尾両生類の系統関係および分岐年代推定）

井川 武

2. 公表論文

(1) Molecular phylogenetic relationship of toads distributed in the Far East and Europe inferred from the nucleotide sequences of mitochondrial DNA genes.
Takeshi Igawa, Atsushi Kurabayashi, Midori Nishioka, M. Sumida
Molecular Phylogenetics and Evolution, 38 (2006) 250 – 260

(2) Complete mitochondrial genomes of three neobatrachian anurans: A case study of divergence time estimation using different data and calibration settings.
Takeshi Igawa, Atsushi Kurabayashi, Chisako Usuki, Tamotsu Fujii, Masayuki Sumida
Gene, 407 (2008) 116 – 129

3. 参考論文

(1) Evolutionary relationships and reproductive isolating mechanisms in the rice frog *Fejervarya limnocharis* complex from Sri Lanka, Thailand, Taiwan and Japan inferred from mtDNA gene sequence analysis, allozyme analysis and crossing experiments.
Masayuki Sumida, Manabu Kotaki, Mohammed Mafizul Islam, Tjong Hon Djong Takeshi Igawa, Yasuyuki Kondo, Masafumi Matsui, De Silva Anslem, Wichase Khonsue, Midori Nishioka
Zoological Science, 24 (2007) 547 – 562

主論文

Genetic divergence of Asian toads and phylogenetic relationships of anuran families (Amphibia, Anura) based on mitochondrial genome information, with special reference to divergence time estimation.

（ミトコンドリアゲノム情報に基づくアジア産ヒキガエル類の遺伝的分化と無尾両生類の系統関係および分岐年代推定）

Takeshi, Igawa

CONTENTS

I. General Introduction

The toads of *Bufo bufo* species group, including the *B. j. japonicus* subspecies group, are widely distributed from the Eurasian continent to the Japanese Archipelago (Inger, 1972; Matsui, 1984). Based on the crossing experiments, Kawamura et al. (1980, 1982) classified the toads from Japan, China and Taiwan as the subspecies group *Bufo japonicus*. According to their reports, this group comprises seven subspecies: *Bufo j. japonicus, B. j. montanus,* and *B. j. torrenticola* from the Japan mainland; *B. j. yakushimensis* from Yaku Isl., Japan; *B. j. miyakonis* from Miyako Isl., Japan; *B. j. gargarizans* from China and Taiwan; and *B. j. bankorensis* from Taiwan. Based on the Morphometric features, however, Matsui (1984) concluded that the Japanese toads are divided into three species and one subspecies: *Bufo japonicus japonicus* and *B. j. formosus, B. gargarizans miyakonis,* and *B. torrenticola.* In a study on the genetic relationships among *Bufo* species and subspecies distributed in the Palearctic and Oriental regions, Nishioka et al. (1990) clarified that the *B. j. japonicus* subspecies group is divided into two groups: the first consisting of the three subspecies *B. j. miyakonis* in Miyako Isl., Japan, *B. j. gargarizans* in China and Taiwan, and *B. j. bankorensis* in Taiwan; the second consisting of four subspecies in the mainland and on Yaku Isl. in Japan. In an examination of the genetic relationships among *B. j. japonicus* populations distributed in the Japanese mainland by allozyme analysis, Kawamura et al. (1990) found that these populations are divided into two major groups, the western and eastern groups.

The *Bufo bufo* species group, therefore, might be expected, like other frog, to provide useful example for studying speciation and/or evolutionary processes caused by paleogeographic events relevant to Eastern Eurasian continent and Japanese island arc. In addition, the *Bufo bufo* species group may also become a possible guide to infer a hypothesis on the evolution of other lineages of non-volant terrestrial vertebrates in this region in the course of its complex geological history. However, the detailed phylogenetic relationships and the process of the geographic distribution of the *Bufo japonicus* subspecies group still remain to be clarified due to the low phylogenetic resolution (by allozyme analyses) and the lack of detailed estimations of divergence times among this frog taxa.

Furthermore, the divergence times of major clades of living amphibians (= lissamphians) are also still controversial. Recently, Zhang et al. (2005a) used mitochondrial (mt) genomic data to estimate the divergence times of major clades of lissamphibians, while San Mauro et al. (2005) also estimated divergence times of lissamphibians by using sequence data of nuclear genes. Both studies used the resultant divergence times to shed light on the early evolution of lissamphibians and the biogeography of major amphibian groups, but their estimations remarkably differed in many respects. According to Lee and Anderson (2006), the discrepancy between these two studies is due to the different calibration methods: Zhang et al. (2005a) applied only a single calibration point, while multiple calibration points were used by San Mauro et al. (2005). However, the divergence time estimation has not been conducted based on mt genome data with multiple calibration points. Finally, the effects of substitution rate,

calibration point setting, and type of data on divergence time estimation have not been studied so far.

In the first part of this study, I carried out phylogenetic analyses based on seven mt genes to elucidate the evolutionary relationships of the *B. japonicus* subspecies group. I also estimated the divergence times of the *Bufo* taxa and discussed possible geologic events to explain the phylogenetic relationship and the current distribution pattern of the toads. In the second part, I determined the complete mtDNA sequences of two hyloid species, *Bufo japonicus* (Bufonidae) and *Hyla japonica* (Hylidae), and one ranoid species, *Microhyla okinavensis* (Microhylidae). Based on these mt genome data, I surveyed structural changes of mtDNAs, and inferred the phylogenetic position of the family Bufonidae among anuran taxa. I also performed divergence time estimations with a variety of sequence datasets and calibration point sets, and surveyed the effects of these factors on branching time estimations.

II. Molecular phylogenetic relationship of toads distributed in the Far East and Europe inferred from the nucleotide sequences of mitochondrial DNA genes.

Abstract

The toads of the *Bufo bufo* species group are widely distributed in the Eurasian continent and Japanese Archipelago. In this study, we analyzed the mtDNA gene sequences of this species group and estimated the divergence time to clarify the evolutionary relationships and biogeography of toads distributed in the Far East and Europe. The phylogenetic tree indicated that this group produced *Bufo bufo* in Europe, whereas it produced *B. japonicus* in the Far East. *B. japonicus* was divided into three major clades corresponding to a group consisting of *B. j. gargarizans* in China, *B. j. bankorensis* in Taiwan, and *B. j. miyakonis* on Miyako Isl. and eastern and western groups of Japanese *B. j. japonicus* subspecies group. The eastern and western groups were divided into several subclades which tended to reflect the region-specific geographic distribution of all localities except *B. j. japonicus* from Hakodate. The estimated branching times of these clades suggest that geological events may have influenced the divergence of the toads distributed in the Far East and Europe.

Introduction

The toads of *Bufo bufo* species group, including the *B. j. japonicus* subspecies group, are widely distributed from the Eurasian continent to the Japanese Archipelago (Inger, 1972; Matsui, 1984). As such, they might be expected, like other frogs, to provide a

useful example for studying speciation and/or evolutionary processes caused by paleogeographic events relevant to Eastern Eurasian continent and Japanese island arc. It may also become possible to infer a hypothesis on the evolution of other lineages of non-volant terrestrial vertebrates in this region in the course of its complex geological history.

Based on the reproductive isolation mechanisms elucidated by crossing experiments, Kawamura et al. (1980, 1982) classified the toads from Japan, China and Taiwan as the subspecies group *Bufo japonicus*. According to their reports, this group comprises seven subspecies: *Bufo j. japonicus, B. j. montanus,* and *B. j. torrenticola* from the Japan mainland; *B. j. yakushimensis* from Yaku Isl., Japan; *B. j. miyakonis* from Miyako Isl., Japan; *B. j. gargarizans* from China and Taiwan; and *B. j. bankorensis* from Taiwan. Based on an analysis of the numerous morphometric features of the Japanese toads, however, Matsui (1984) concluded that the Japanese toads are divided into three species: *Bufo japonicus* (*B. j. japonicus* and *B. j. formosus* synonymized with *B. japonicus japonicus* in present study), *B. gargarizans miyakonis* (synonymized with *B. j. miyakonis* in present study), *B. torrenticola* (synonymized with *B. j. torrenticola* in this study). In a study on the genetic relationships among *Bufo* species and subspecies distributed in the Palearctic and Oriental regions, Nishioka et al. (1990) found that the *B. j. japonicus* subspecies group is divided into two groups: the first, consisting of the three subspecies *B. j. miyakonis* in Miyako Isl., Japan, *B. j. gargarizans* in China and Taiwan, and *B. j. bankorensis* in Taiwan; the second consisting of four subspecies in the mainland and on Yaku Isl. in Japan. In an examination of the genetic relationships

among *B. j. japonicus* populations distributed in the Japanese mainland by allozyme analysis, Kawamura et al. (1990) found that these populations are divided into two major groups, the western and eastern groups. This grouping corresponds to *B. j. japonicus* and *B. j. formosus* designated by Matsui (1984). However, the molecular phylogenetic relationships and the process of the geographic distribution of the *Bufo japonicus* subspecies group remain to be clarified due to the limited number of polymorphic loci and the lack of informative markers for divergence time.

Mitochondrial DNA can be a powerful molecular marker for reconstructing evolutionary lineages in animals (Avise, 1994; Kocher and Stepien, 1997). Many recent phylogenetic studies have also applied mitochondrial DNA markers to infer the histories of animals with respect to geography, geology, and paleoclimatology (Macey et al., 1998; Mulcahy and Mendelson, 2000). We thus used mtDNA gene sequence data in phylogenetic analysis to elucidate the evolutionary relationships within the *B. japonicus* subspecies group. Finally, we estimated the divergence times of *Bufo* taxa based on the mtDNA data and discussed possible geologic events believed to explain the current distributions of these toads.

Materials and methods

Specimens. We analysed 33 *Bufo* individuals in total consisting of 30 *B. japonicus* from different populations, one *B. bufo*, one *B. viridis* and one *B. americanus*. The collecting stations were shown in Table 1 and Fig. 1. Taxonomic status were followed as previously published (Kawamura et al., 1990; Nishioka et al., 1990), and accordingly, *B.*

japonicus was divided into six subspecies (see Table 1).

DNA sequencing. Total DNA was extracted from clipped toe, liver or muscle samples of each toad specimen using the Qiagen DNEasy tissue extraction kit according to the manufacturer's instructions. The total DNA was used for amplifying DNA fragments by polymerase chain reaction (PCR) with a set of primers for cytbF1/bufo and R51 (Appendix A). PCR mixtures were prepared with an LA-Taq Kit (TaKaRa) according to the manufacturer's protocol. The resulting fragments were amplified by 35 shuttle PCR cycles consisting of denaturation for 20 sec at 98°C followed by annealing and extension for 5 min at 60 °C. The amplified DNA fragments were approx. 6 kbp in length and corresponded to nucleotide positions 16869–17802 and 1-5149 of the complete mitochondrial DNA sequence of the frog species *Rana nigromaculata* (Sumida et al., 2001, GenBank Accession No. AB043889) (contains Cyt *b*, D-loop, tRNA-Leu(CUN), tRNA-Thr, tRNA-Pro, tRNA-Phe, 12S rRNA and 16S rRNA genes in *Bufo japonicus* (our unpublished data)). The PCR fragments were purified with PEG precipitation (Kraft et al., 1988) then partial portions of the Cyt *b*, 12S rRNA, and 16S rRNA genes and four entire tRNA (Leu(CUN), Thr, Pro, and Phe) genes were directly sequenced with each primer (Appendix A) using a cycle sequencing kit (DYEnamic ET dye terminator, Amersham) and automated DNA sequencer (ABI 373A, Applied Biosystems). The resultant sequences were deposited in the EMBL/GenBank/DDBJ database (Table 1).

Phylogenetic analyses. The resultant Cyt *b*, tRNAs, 12S rRNA, and 16S rRNA gene sequences from the 33 *Bufo* specimens were aligned using the ClustalW program (Thompson et al., 1994). Initially, we obtained alignment data for each gene region then eliminated any ambiguous and gap sites by observation. To survey the phylogenetic utilities of the different gene regions, we used these data for further phylogenetic analyses. Furthermore, we made a combined data consisting of all four alignment data to construct total evidence tree. Before combining four data sets, we conducted an ILD test for all possible combinations using the partition homogeneity test (parsimony method of Farris et al., 1995) implemented in PAUP* 4.0b10 (Swofford, 2002) to check whether all of the sequences were suitable for combination. The alignment data used in this study are available at: http://home.hiroshima-u.ac.jp/amphibia/sumida/bufoaln.

Maximum likelihood (ML), maximum parsimony (MP), and neighbor joining (NJ) analyses for all five data sets were carried out using PAUP*. In all cases, *B. americanus* was used as the outgroup. The ML and NJ analysis was conducted using substitution models and parameters estimated by Modeltest version 3.06 (Posada and Crandall, 1998). The proposed model for each data set was denoted in Table 2. The reliabilities of the resultant trees were evaluated by Bootstrap statistics (BP). BP values were calculated by 1000 replications in the MP and NJ optimality criterion and by 100 replications in the ML analysis.

Estimating the date of divergence. The divergence times of the Japanese *Bufo* taxa were estimated from all usable alignments sites (2073 sites) based on the Bayesian

relaxed molecular clock method using MultiDivTime version 9/25/03 (Thorne and Kishino, 2002). First, we separately estimated the model parameters for each alignment data set (Cyt *b*, four tRNAs, 12S, and 16S) using the baseml program in the PAML package (Yang, 1997). The resultant parameters were used to estimate the branch lengths with the estbranches program in the MultiDivTime package (Thorne and Kishino, 2002). Following this, we performed MCMC analysis to approximate the posterior distribution rates and divergence times based on the topology of the combined analysis (Fig. 2A) using multidivtime in the MultiDivTime package. In this analysis, an internal node between the Asian clade and *B. bufo* was saved as a fixed reference point for comparison of the relative divergence ages; the branching date, 10 Ma, was previously reported by Macey et al. (1998). A paleogeographical event, aridization of Central Asia caused by uplifting of the Himalayas was also reported to have occurred 10 Ma (Harrison et al., 1992).

Results

Nucleotide sequences. Nucleotide sequences were determined for partial portions of the Cyt *b*, 12S rRNA, and 16S rRNA genes and four complete tRNA (Leu(CUN), Thr, Pro, Phe) genes from 33 *Bufo* taxa. Four sets of alignment data were obtained with the resultant sequences. The alignment data is summarized in Table 1. We checked for saturated substitutions in each data set by plotting transition/transversion ratio. Although the Cyt *b* sequence seemed to show a weak saturated substitution pattern, the four tRNA, 12S, and 16S sequences showed no saturation.

Figure 2 shows the mean nucleotide divergences (with uncorrected P values) of the sequenced genes at each taxonomic level. The magnitudes of divergence were correlated to the taxonomic level for all genes examined.

The partition homogeneity test (Farris et al., 1995) revealed that all four alignment data sets were suitable for combination (homogeneity not rejected, $P = 0.93$). Thus, we obtained a combined alignment data containing all sequenced portions (see Table 2) and used this in addition with the four individual alignment data sets in subsequent phylogenetic analyses.

Phylogenetic analyses. The results of phylogenetic analyses based on each data set are summarized in Table 3. Similar phylogenetic trees were reconstructed for all data sets used. The BP values varied considerably across data sets; however, the combined data tended to provide higher bootstrap values than the individual data (Table 3). Therefore, we mainly describe the phylogenetic relationships based on the combined data.

Figure 2A shows a single ML tree ($-\ln L = 7707.14526$) obtained from the combined data. *Bufo bufo*, the continental and Taiwanese toads (*B. j. gargarizans,* and *B. j. bankorensis*), and all of the Japanese toads (*B. j. japonicus, B. j. montanus, B. j. torrenticola, B. j. yakushimensis,* and *B. j. miyakonis*) in this tree formed a clear monophyletic group (clade 1, BP: 100). Within the *Bufo bufo* species group (corresponding to clade 1 in Fig. 2A), *B. bufo* was placed in the basal position and the other taxa were divided into three major groups (clades 4, 5, and 11) supported by high

BP values (> 95%) (see Table 3). One of these three groups, clade 11 consisting of *B. j. miyakonis*, *B. j. bankorensis*, and *B. j. gargarizans*, was initially included as a sister group of the other Japanese *Bufo* taxa. The localities of the initially divided taxa (Miyako Isl., Taiwan, and China) are separate from the Japan mainland. The *Bufo* taxa living on the Japan mainland (*B. j. japonicus*, *B. j. montanus*, *B. j. yakushimensis*, *B. j. torrenticola*) formed a clear monophyletic group, clade 3, which was subdivided into two major groups with high BP values (> 96%), clades 4 and 5. Clade 5 corresponded to the eastern Japan group and consisted of *B. j. japonicus* and *B. j. montanus*, while clade 4 corresponded to the western Japan group and consisted of *B. j. japonicus*, *B. j. torrenticola*, and *B. j. yakushimensis*.

These eastern and western clades were each further divided into three subclades supported by high BP values (>90%). The eastern group (clade 5 in Fig. 2A) was divided into three subclades corresponding to three areas of eastern Japan: clade 8, central (Kanto and Tokai districts), clade 9, northern (Tohoku district); and clade 10, northeastern (Kanto and Tohoku districts, excluding Hakodate). Similarly, the western group (clade 4) was divided into three subclades corresponding to areas of western Japan: clade 15, central (Kinki, Chugoku, and Shikoku districts); clade 16, comprising two populations of *B. j. torrenticola*; and clade 17, southern (Kyushu district, including Yaku Island). These phylogenetic relationships closely matched the geographic distribution pattern in all but one case; namely, *B. j. japonicus* from Hakodate. Although the Hakodate is situated in the northernmost area of the *B. j. japonicus* distribution, *B. j. japonicus* from Hakodate was included in the eastern group (clade 10) rather than the

northern group (clade 9).

Estimating the date of divergence. Divergence ages of the Asian *Bufo* taxa were estimated by Bayesian molecular dating. In this analysis, we used the divergence time between *B. bufo* and the Asian clade (Macey et al., 1998) as a fixed reference divergence point (10 Ma of clade 1 in Fig. 2B). The resultant ultrametric tree based on the ML topology and estimated divergence time of the *Bufo* taxa are shown in Fig. 2B. The estimated date of divergence was well matched to the proposed geological date.

To check the relevancy of the fixed reference point used above and the resultant divergence times, we carried out an additional divergence time estimation. In this analysis, we used the linearized tree method implemented in MEGA2.1 (Kumar et al., 2001), because this method requires no hypothetical reference divergence point. The NJ tree obtained from the combined data was used as the basal tree in the branch length linearization.

Discussion

Phylogenetic relationships and taxonomic implications. Our phylogeny indicated that the *B. japonicus* taxa examined here have a closer common ancestor with European *B. bufo* than *B. viridis*. This seems to support the hypothesis recognizing these species as members of the *Bufo bufo* species group based on morphology (Inger, 1972). Our result also matches the results from karyology (Matui, 1980) and allozyme analysis (Nishioka et al., 1990).

All our analyses strongly support the monophyly of *B. j. japonicus* subspecies group, corresponding to the results of previous crossing experiments (Kawamura et al., 1980, 1982). In these previous analyses, all hybrids between the *B. j. japonicus* subspecies group were fertile, while male hybrids between *B. bufo* and the *B. j. japonicus* subspecies group were sterile.

The resultant trees showed that the *B. j. japonicus* subspecies group was divided into three major clades. In the initial divergence, the ancestors of the clade consisting of *B. j. gargarizans, B. j. bankorensis,* and *B. j. miyakonis* from the China, Taiwan and Miyako Isl. diverged from another clade consisting of *B. j. japonicus* from the Japan mainland. This was followed by further divergence into eastern and western groups. These divergences were in agreement with three clusters detected by allozyme analyses (Nishioka et al., 1990; Kawamura et al., 1990). Morphometric analyses also agree with these relationships. Matsui (1984) divided Japanese common toads (*B. j. japonicus* in this study) into two subspecies (*B. j. formosus* and *B. j. japonicus*) based on their morphology; these two subspecies roughly correspond to the eastern and western groups in our study. Within these eastern and western groups, our results identified subclusters that tended to reflect a region-specific geographic distribution similar to those found by allozyme analyses (Nishioka et al., 1990; Kawamura et al., 1990).

Although Hakodate is located near Tohoku (Fig. 1), the Hakodate population was exceptionally grouped with several Kanto populations rather than the Tohoku populations (clade 10 in Fig. 2A). Furthermore, pairwise sequence divergence between the Hakodate and Kashiwa (one population from Kanto) populations was the lowest

(Cyt *b*: 0.0230, tRNA: 0.0000, 12S: 0.0049, 16S: 0.0039, and combined data: 0.0019) of all the pairwise divergences identified (from 0.0019 to 0.1410 between *B. bufo* and *B. americanus*, mean = 0.0569). Noting the same disjunct distribution in a separate study using allozyme data, Kawamura et al. (1990) postulated that some *B. j. japonicus* toads were artificially introduced into Hokkaido from the Kanto district surrounding Tokyo Bay. Furthermore, Matsui (1984) suggested that the morphometric value of the Hakodate population completely overlapped those of the Yokohama population near Kashiwa. Although the small genetic divergence between the Hakodate and Kashiwa populations could be explained by such as the presence of ancestral polymorphism and/or incidental similar nucleotide sequences due to quite low genetic divergences among eastern *B. japonicus* populations, our findings and previous knowledge support the artificial introduction scenario.

Matsui (1976) designated the Japanese stream toad (*B. j. torrenticola* here) a new species (*B. torrenticola*) based on morphological and ecological observations; however our present analysis and previous allozyme analysis (Kawamura et al., 1990) reveal that the Japanese stream toad forms one of the subgroups within the western group of *B. j. japonicus*. However, the detailed position of *B. j. torrenticola* in the western group was not resolved by the present study. Both Kishino-Hasegawa (1989) and Shimodaira-Hasegawa (1999) tests did not reject the topologies (*B. j. torrenticola* + all western *B. j. japonicus*) and (*B. j. torrenticola* + western *B. j. japonicus* from Arashi to Nichinan) at $P < 0.05$. Thus, further studies are required to clarify whether *B. j. torrenticola* is one of the western *B. j. japonicus* subgroups.

Divergence time and biogeography. The *Bufo* taxa used in our study were broadly divided into seven clades. These groupings basically agreed with previous allozyme analysis and morphological studies; studies in which the authors were unable to discuss the biogeographical hypotheses for the *B. j. japonicus* subspecies group due to a lack of molecular clocks. However, in the present study, no fossil records were available to identify the branching times between Japanese and Asian continental *Bufo* taxa. Accordingly, we used a molecular timescale calibrated with geographic evidence presented by Macey at al. (1998) who indicated that the European and Asian *Bufo* species split occurred 10 Ma. The divergence between the *B. japonicus* subspecies and European common toad *B. bufo* was estimated to have taken place with uplifting of the Transhimalaya and Tibetan Plateau, which effectively dried out Central Asia by blocking the Indian monsoons (Harrison et al., 1992) (Fig. 4B). A similar branching pattern between European and Asian taxa in this era was also reported for the pond frog (*Rana*) species group (Sumida et al. 2000) with an estimated divergence at around 10 Ma.

As shown in Fig. 2B, the following divergence times were obtained from Bayesian molecular dating: (1) 6.8 ± 0.9 Ma between the Chinese, Taiwanese and Miyako Isl. and Japanese clades (clade 2 in Fig. 2B), (2) 5.7 ± 1.0 Ma between the eastern and western groups on the Japan mainland (clade 3 in Fig. 2B), (3) 4.4 ± 1.0 Ma for the several western subgroups (clade 4 in Fig. 2B), and (4) 3.6 ± 1.0 Ma for the several eastern subgroups (clade 5 in Fig. 2B). On the basis of these estimations, we inferred the

biogeographic events that caused the main branchings of the *Bufo* groups. Initial branching between eastern continental and Japanese toads was estimated to have occurred in the Late Miocene (Fig. 2B, clade 2). Takehana et al. (2003) estimated branching of the freshwater fish *Oryzias latipes* at almost the same date. This branching took place during the same era when the Philippine Sea plate (PHS) resumed its subduction (Kamata, 1999; Kamata and Kodama, 1994; Itoh and Nagasaki, 1996). The PHS subduction caused two distinct geologic events: the formation of a large volcano-tectonic depression in the center of Kyushu district and back-arc spreading of the Ryukyu Arc (Fig. 4C). The stock of Japanese *Bufo* species dispersed from the continent through the land bridge from the Korean Peninsula to the Japanese Archipelago (Hikida et al., 1989). The geographic events that occurred in the Kyushu district and Ryukyu Arc might have broken this land bridge and played a critical role in isolating the ancient Japanese *Bufo* species from continental species.

Our findings suggested that *B. j. miyakonis* was divided from the continental *B. j. gargarizans* and Taiwanese *B. j. bankorensis* in the Pleistocene era at approx. 0.9 Ma and 1.3 Ma, respectively. The oldest fossil record of *B. j. miyakonis* from the Late Pleistocene (< 1 Ma) deposit on Miyako Island (Nokariya and Hasegawa, 1985) seems to agree with the result. Furthermore, no native populations or fossil records of the genus *Bufo* have ever been found in the other Ryukyu Islands (Ota, 2003). Our results and the *Bufo* distribution pattern seem to support the hypothesis that the disjunction between Miyako Island and the other Ryukyu Islands (approx. 6 Ma, Late Miocene) preceded the fragmentation of Miyako Island and the Eurasia continent/Taiwan (approx.

1 Ma, Pleistocene) (Ota, 1998). A similar distribution pattern and divergence have also been reported for the lizard *Takydromus toyamai* (Ota et al., 2002) and snakes *Amphiesma concelarum* and *Calamaria pfefferi* (Ota, 1998).

The Japanese *Bufo* species diverged into two major groups (eastern and western) in the Early Pliocene (5.7 Ma) after separation from the Asia continental species (clade 3 in Fig. 2B). Similar geographical divergence patterns have also been observed in other frogs such as *Rana rugosa* (Nishioka et al., 1993) and *Buergeria buergeri* (Atsumi et al., 1998; Sumida et al., 2004). These findings suggest that divergence among these frog species might have been brought about by the same geographic event. An event corresponding to expansion of this ancient basin might have caused divergence between the western and eastern Japan in the Early Pliocene (Fig. 4D). For example, many basins expanded in an intra-arc depressional zone called the Setouchi Geologic Province and in the back arc area of a mainland known as the Green Tuff region (Itoigawa, 1991; Yoshida, 1992; Kuwahara, 1985). These basins might have segmented the distribution range of the ancestral Japanese *Bufo* species.

There are several possible phylogenetic positions for *B. j. torrenticola* as mentioned above; however, all possible topologies support the grouping of *B. j. torrenticola* and western *B. j. japonicus*. Thus, the morphological appearance of this subspecies seems to have developed after divergence from eastern *B. j. japonicus* (< 5.7 Ma). The distribution range of this subspecies is limited to a mountainous area near the border of the two major groups, western and eastern. As mentioned above, the ancient basin expanded to these areas during the Early Pliocene followed by a period of uplifting and

volcanic activity, which transformed the neighboring landmass in the Pliocene (Takeuchi, 1999a, b). The mountains, basins, and other geographic features in this area might have restricted dispersal of *B. j. torrenticola* from this mountainous area, thereby isolating this subspecies and setting the stage for morphological differentiation.

In conclusion, we showed that the branching dates estimated from mtDNA data are closely related to the geographic history of the Eurasian continent and Japanese Archipelago. We point out, however, that the fossil records and specimens used to identify the branching time in this study were somewhat limited. Consequently, Eurasia and the Japanese Archipelago might be attractive areas for combining phylogenetic and biogeographic studies. Further molecular analyses and fossil records are necessary to provide deeper insight into the evolutionary history of the *B. j. japonicus* subspecies group and *B. bufo* species group.

III. Complete mitochondrial genomes of three neobatrachian anurans: A case study of divergence time estimation using different data and calibration settings.

Abstract

We sequenced the whole mitochondrial (mt) genomes of three neobatrachian species: Japanese tree frog *Hyla japonica,* Japanese common toad *Bufo japonicus*, and narrow-mouthed toad *Microhyla okinavensis*. The gene arrangements of these genomes diverged from that of basal anurans (suborder Archaeobatrachia), but are the same as that of the members of derived frogs (i.e., superfamily Hyloidae and Ranoidae in suborder Neobatrachia), suggesting the one-time occurrence of a gene rearrangement event in an ancestral lineage of derived anurans. Furthermore, several distinct repeat motifs including putative termination-associated sequences (TASs) and conserved sequence blocks (CSBs) were observed in the control regions (CRs) of *B. japonicus* and *H. japonica*, while no repeat motifs were found in that of *M. okinavensis*. Phylogenetic analyses using both nucleotide and amino acid data of mt genes support monophyly of neobatrachians. The estimated divergence time based on amino acid data with multiple reference points suggests that the three living amphibian orders may have originated in the Carboniferous period, and that the divergences of anurans had occurred between the Permian and Tertiary periods. We also checked the influence of the data types and the settings of reference times on divergence time estimation. The resultant divergence times estimated from several datasets and reference time settings suggest that the

substitution saturation of nucleotide data may lead to overestimated (i.e., older) branching times, especially for early divergent taxa. We also found a highly accelerated substitution rate in neobatrachian mt genes, and fast substitution possibly resulted in overestimation. To correct this erroneous estimation, it is efficient to apply several reference points among neobatrachians.

Introduction

Vertebrate mitochondrial DNA (mtDNA) is a closed circular molecule. The genome organization is highly compact, and the genome is approximately 16 kbp in length (Wolstenholme, 1992). This genome typically contains 37 genes for 2 ribosomal (r)RNAs, 22 transfer (t)RNAs and 13 proteins, and a long noncoding region called the control or D-loop region that includes signals required for regulating and initiating mtDNA replication and transcription (Wolstenholme, 1992; Sbisà et al., 1997).

Mitochondrial gene arrangements are generally conserved in vertebrates. All 37 genes are arranged in the same relative order in almost all vertebrate species from teleost fishes to eutherian mammals (Anderson et al., 1981; Roe et al., 1985; Tzeng et al., 1992; Boore, 1999), though some taxa has rearranged mt gene orders [e.g., in marsupials, birds, reptiles, lampreys, and fishes (see Boore 1999)]. As for amphibians, however, mitochondrial gene rearrangements have been found in a number of taxa. For example, tRNA gene rearrangements were observed within closely related South American caecilians (San Mauro et al., 2006). In Caudata, gene rearrangements and duplication of genes or control regions were also found in mtDNAs of plethodontid

salamanders (Mueller and Boore, 2005). In anurans, the mt gene arrangements of basal groups (archaeobatrachians) are completely identical to those of typical vertebrates (Roe et al., 1985; San Mauro et al., 2004; Gissi et al., 2006). However, in hyloid and ranoid frogs in the phylogenetically nested anuran group (suborder Neobatrachia), the gene arrangement diverged from the typical one. In most neobatrachian mtDNAs, four tRNA genes translocated from typical positions, and these tRNA genes formed a cluster upstream of the 12S rRNA gene (LTPF tRNA cluster; Sumida et al., 2001; Zhang et al., 2005a). In addition, further gene rearrangements have been reported in a major neobatrachian clade, the epifamily Ranoidae. Within Ranoidae, complete mtDNA sequences of six species have been reported so far (Sumida et al., 2001; Sano et al., 2004, 2005; Zhang et al., 2005b; Liu et al., 2005; Kurabayashi et al., 2006) and five of these except *R. nigromaculata* possess additional rearrangements that are different from each other. Especially, mtDNAs of genus Madagascan frogs (genus *Mantella*) show extended rearrangements (Kurabayashi et al., 2006). In addition, the neobatrachian mt genomes vary in length ranging from about 16 kbp (*Microhyla heymonsi*) to 23 kbp (*Mantella madagascariensis*). The size variations of neobatrachian mtDNA are mainly caused by length differences of D-loops, which usually contain long and many repeated sequences. These many instances of gene rearrangements make neobatrachian frogs an excellent model for examining the mechanisms of such vertebrate mitochondrial instability. Although a number of complete mtDNAs have been reported in Ranoidea, only two complete mtDNAs of *Hyla chinensis* and *Bufo melanostictus* (Zhang et al., 2005a) have been reported in superfamily Hyloidea, the other major taxon of

neobatrachia. In this study, we determined the complete mtDNA sequences of two hyloid species, *Bufo japonicus* (Bufonidae) and *Hyla japonica* (Hylidae), and one ranoid species, *Microhyla okinavensis* (Microhylidae). Based on these data, we surveyed structural changes of mtDNAs among phylogenetically closely related species in anurans.

Furthermore, mt genomes have been used for phylogenetic analyses and divergence time estimations. Zhang et al. (2005a) used mt genome data to estimate the divergence times of major clades of living amphibians (= lissamphibians), while San Mauro et al. (2005) also estimated divergence times of lissamphibians by using sequence data of nuclear genes. Both studies used these estimated divergence times to shed light on the biogeography of early lissamphibians and major amphibian groups, but their estimated divergence times remarkably differed in many respects. According to Lee and Anderson (2006), the discrepancy between the two studies is due to the use of different calibration methods: Zhang et al. (2005a) applied only a single calibration point, while multiple calibration points were used by San Mauro et al. (2005). However, the divergence time estimation has not been conducted based on mt genome data with multiple calibration points. Finally, the effects of substitution rate, calibration point setting, and type of data on divergence time estimation have not been studied so far. Thus in the present study, we performed divergence time estimations with a variety of mitochondrial data and calibration point sets, and surveyed the effects of these factors on branching time estimations.

Materials and Methods

DNA sources. We used three anuran species: Japanese common toad *B. japonicus*, Japanese tree frog *H. japonica*, and narrow-mouthed toad *M. okinavensis*, as representatives of three neobatrachian families, Bufonidae, Hylidae, and Microhylidae, respectively. *Bufo japonicus* was collected in Yoshiwa, Hiroshima and the specimen has been kept at –80 °C in the Institute for Amphibian Biology of Hiroshima University (IABHU voucher no. 4001). *Hyla japonica* was collected in Ushita, Hiroshima (IABHU voucher no. 6123). *Microhyla okinavensis* was collected in Ishigaki Island, Okinawa (IABHU voucher no. 5263). The total genomic DNA was extracted from a clipped toe of each specimen using the DNeasy® Tissue Kit (QIAGEN).

PCR and sequencing. For each species, the complete mt genome was sequenced. Firstly, we amplified overlapping fragments that covered the entire mt genome by normal PCR or long-and-accurate (LA) PCR methods (Fig. 5). TaKaRa Ex- and LA-Taq™ Kits were used for normal and LA PCR reactions, respectively. The conditions of the PCR reaction followed the manufacturer's instructions. The resultant fragments were purified by polyethylene glycol precipitation (Kraft et al., 1988) or gel extraction. For gel extraction, the fragments were electrophoresed on 0.7% agarose gel and the target DNAs were purified from excised pieces of gel using Gen Elute Agarose Spin Column (Sigma). In principle, the primer walking method was employed to sequence the amplified fragments (the walking primers used are available from the authors upon request). To make internal walking primers, long PCR fragments (fragment E of *H.*

japonica and fragment O of *M. okinavensis* in Fig. 5) were digested by *Hinc* II and *Hind* III and resultant fragments were subcloned into pUC118 *E. coli* vector using T4 DNA ligase according to a standard protocol (Sambrook and Russell, 2001). DNA sequencing was performed using automated DNA sequencers (373A and 3100-*Avant,* ABI) with the DYEnamic™ ET Terminator Cycle Sequencing Kit (GE Healthcare) or BigDye® Terminator Cycle Sequencing Kit (Applied Biosystems). Two PCR fragments (fragment A of *B. japonicus* and fragment F of *H. japonica* in Fig. 5) containing long tandem repeats where we could not design walking primers were subcloned into pCR® 2.1 vector by using the TOPO TA Cloning® Kit (Invitrogen). To determine the precise sequence of long tandem repeats found in the control regions, series of deleted subclones were made from the resultant clones using the Exonuclease III deletion method (Henikoff, 1987). From the PCR fragments and subclones, the entire mtDNAs of three species were sequenced.

Sequence data were analyzed with GENETIX (Software Development) and DNASIS (Hitachi Software Engineering). Genes were identified by comparison with corresponding gene sequences from other vertebrates, and also, in the case of tRNA genes, by determination of secondary structural features. The complete sequences of *B. japonicus*, *H. japonica*, and *M. okinavensis* mtDNAs were deposited in the Genbank/EMBL/DDBJ database, accession number AB303363, AB303363, and AB303950, respectively.

Sequence alignments. In addition to our sequenced data, we used mt genome data

information from 29 vertebrates: 14 frogs, four salamanders, three caecilians, a crocodile, a bird, two mammals, and two fishes (Table 4). The sequence data of *Xenopus laevis* (M10217, Roe et al., 1985) is suspected to contain a number of sequencing errors in the 12S rRNA gene, so we used another 12S rRNA gene sequence of this species (M27605, Dunon-Bluteau and Brun, 1986).

For phylogenetic analyses and divergence time estimation, we prepared three multiple alignment data sets. (1) Concatenated amino acid data, 3,197 aa from 12 protein genes. (The data of ND6 gene were not used because this gene is encoded by the *L*-strand and has different nucleotide composition bias, accordingly different amino acid composition bias, from the other 12 protein encoding genes). (2) Concatenated nucleotide data, 9,591 bases corresponding to the above 3,197 aa and 1,383 bases from two rRNA genes. (3) Concatenated nucleotide data of two rRNA genes and 1st and 2nd codon sites of the 12 protein genes (i.e., minus codon 3rd positions from data set 2). Data sets 1 and 2 were used for both the phylogenetic analyses and the time estimation, while data set 3 was used only in the branching time estimation. Data set 3 reconstructed the same tree topology these from data set 1 and 2. Thus, we only describe the results of phylogenetic analyses based on data set 1 and 2. (But we supplied phylogenetic trees from a –3rd codon nucleotide data set including *Ascaphus* and *Pelobates* in Fig. 8). To make the alignment data, firstly we aligned the amino acid sequence of each protein-coding gene by Clustal X (Thompson et al., 1997) with the default setting. Then we eliminated poorly aligned sites using GBlock (Castresana, 2000) with default parameters. Nucleotide sequences of rRNA genes were aligned in the

same manner. Then, we concatenated the amino acid data from 12 protein genes and the nucleotide data from the 12 protein and two rRNA genes.

Phylogenetic analysis. Phylogenetic analyses were conducted with data sets 1 and 2 using the maximum likelihood (ML), Bayesian inference (BI), and maximum parsimony (MP) methods. The ML analyses were performed using PHYML Ver. 2.4.4 (Guindon and Gascuel, 2003). MrBayes Ver. 3.0b4 (Huelsenbeck and Ronquist, 2001) was used for BI analyses. For BI analyses, the following settings were used: number of Markov chain Monte Carlo (MCMC) generations = 1.5 million, and sampling frequency = 10. The burn-in sizes for both amino acid and nucleotide data were determined by checking convergences of –log likelihood (–ln*L*) values using the AWTY program (Wilgenbusch et al., 2004), and the first 150,000 generations were discarded. All MCMC runs were repeated twice to confirm consistent approximation of the posterior parameter distributions. In the ML and BI analyses, we applied the general time-reversible (GTR; Rodriguez et al., 1990) model with gamma (G) distribution (with 8 categories) and proportion of invariable site (I) for nucleotide data, and the mtREV model (Adachi and Hasegawa, 1996) with G (8 categories) was used for amino acid data. These substitution models were suggested from Akaike information criteria implemented in Modeltest 3.06 (Posada and Crandall, 1998) and ProtTest 1.3 (Abascal et al., 2005). Robustness of the resultant ML trees was calculated using nonparametric bootstrap probabilities (BPs) with 200 pseudo-replications, and statistical support of the resultant BI trees was evaluated by the Bayesian posterior probability (BPP). The MP

analyses were performed based on amino acid and nucleotide data by using PAUP*4.0b10 (Swofford, 2003). The robustness of the MP trees was also evaluated by BPs with 1,000 resamplings.

Estimation of divergence time. Divergence times were determined using the Multidivtime software package (Thorne and Kishino, 2002; available from http://statgen.ncsu.edu/thorne/). This software was implemented using a Bayesian approach that incorporated the variations of substitution rates among genes and among lineages (Thorne et al., 1998; Kishino et al., 2001; Thorne and Kishino, 2002). Following the instructions of the software, the topology resulting from previous ML and BI analyses based on both amino acid and nucleotide data was used as the initial tree. We used F84 substitution model for all nucleotide data (data sets 2 and 3) according to the instruction of Multidivtime. For amino acid data (data set 1), we used mtREV-F24 model was used following the methods of Armer and Kumazawa (2005). We also optimized parameters for these models using PAML (Yang, 1997) (for mtREV-F24 model, modified version of CODEML was used; available from ftp://statgen.ncsu.edu/pub/thorne/Kumazawa.tgz). The branch lengths of the initial tree and divergence times were estimated using the programs Estbranches and Multidivtime in the Multidivtime package. The Bayesian method also required the specification of prior distributions of branching times (i.e., fixed reference points). The prior assumption of the ingroup root node was set to 400 Ma (rttm = 400) with standard deviation of 10 Ma (rttmsd = 10). We also introduced fossil records and other usable branching time

evidences as fixed reference points (Table 5). Unlike recent molecular time estimation (San Mauro et al., 2005; Roelants et al., 2007) in which one-hand (only minimum or maximum limit) time constraints were used, we applied both minimum and maximum limits for many calibration points. The differences of reference points between this study and previous papers are summarized in Table 5.

To assess the influence of reference points in divergence time estimation, three estimations with different combinations of reference point setting were performed for each data set (see Table 5): (1) all 7 reference points (ref-set 1), (2) 6 reference points except the branching between Rhacophoridae and Mantellidae (73.1 ± 19.5 Ma = youngest one) (ref-set 2), and (3) 6 reference points except Amniota from the calibration point between diapsids and synapsids (310 ± 10 Ma = oldest one) (ref-set 3). The Markov chain Monte Carlo (MCMC) method was employed to permit approximation of posterior distributions (Kishino et al., 2001). Initial parameter values were randomly selected to initialize the Markov chain, and then a burn-in period of 100,000 cycles was completed before parameters were sampled from the MCMC chain. Afterward, the state of the Markov chain was sampled every 100 cycles until a total of 200,000 generations.

Results and Discussion

Genome composition. The complete mt genomes of three neobatrachian species, *B. japonicus, H. japonica,* and *M. okinavensis,* were sequenced. All three mt genomes encoded 37 typical mt genes (i.e., 13 protein, two rRNA, and 22 tRNA genes), and all of these genes were similar in length to their counterparts in other anurans. Contrary to

this, the genome sizes of these three mtDNAs highly diverged, ranging from 16,717 (*M. okinavensis*) to 19,519 bp (*H. japonica*) (Table 6). These differences were caused by length differences in their control regions (Fig. 6). In *B. japonicus* and *H. japonica* mtDNAs, the control regions possessed two tandem repeats at both 5' and 3' ends, and these repeats made long control regions (2,351 bp and 4,103 bp, respectively). In contrast, the control region of *M. okinavensis* did not include repeat units and its length was 1,335 bp (Fig. 6).

When we compared the structures of the control regions among closely related species, most features were shared within the same genus (Fig. 6). For *Bufo* species, the control regions of *B. japonicus* and *B. melanostictus* commonly possessed repeat motifs at both 5' and 3' ends. The 3' repeats of these species consisted of three repeat units of 102 – 103 bp (plus one incomplete unit of 36 bp) and showed high sequence similarity (rep. B and D). Although the number and length of 5' repeats differed between the two species (*B. japonicus* possessed three repeats of 207 – 227 bp [rep.A] and *B. melanostictus* two repeats of 86 bp [rep.C]), the 3' part of rep.A showed high sequence similarity with rep.C. Furthermore, in both species, the 5' repeat motifs contained two putative termination-associated sequences (TASs) and the 3' repeat motifs possessed two conserved sequence blocks (CSB-2 and CSB-3). Similarly, in *Hyla* species, the control regions of *H. japonica* and *H. chinensis* possessed 5' repeat motifs (rep.E and G) including TAS. Two *Hyla* species also had repeat motif(s) at the 3' end of the control region. However, these 3' repeats differed in both nucleotide sequence and structural feature. The *H. chinensis* control region had two distinct 3' repeat motifs

(rep.I and H), and one motif (rep.H) contained CSB-2 and CSB-3, as found in *Bufo* species, while the control region of *H. japonica* possessed only one repeat motif at the 3' end and this motif did not contain CSBs. Usually, CSBs are not included in repeat motifs (e.g., San Mauro et al., 2004). However, CSB-2 and CSB-3 included in repeats have been observed in three *Bufo* and *Hyla* species reported so far. This suggests that the presence of the CSBs in repeat motifs is an ancestral state that originated in a common ancestor of these two genera. In this context, the *H. japonica* CSBs not included in a repeat motif seem to be a derived condition in this taxon. For microhylids, no obvious repeat motifs were found in the control region, which is the chief factor responsible for the relatively short control region. Microhylid control regions without any repeat motif are unusual, because almost all anuran control regions contain several repeat motifs, particularly, in most reported mtDNAs from superfamily Ranoidae: *Rana nigromaculata* (Sumida et al., 2001), *Buergeria buergeri* (Sano et al., 2004), *Rhacophorus schlegelii* (Sano et al., 2005), and *Mantella madagascariensis* (Kurabayashi et al., 2006). Therefore, the microhylid control regions lacking repeat sequences seem to be a synapomorphy originating in a common ancestor of this family.

In the mtDNAs analyzed here, the tRNA-Leu (CUN), tRNA-Thr, tRNA-Pro, and tRNA-Phe genes were located upstream of the 12S rRNA gene and formed a tRNA gene cluster (LTPF tRNA cluster). This tRNA gene arrangement is different from that of typical vertebrates including basal anurans (archaeobatrachians) (San Mauro et al., 2005; Zhang et al., 2005a; Gissi et al., 2006). However, hyloid and ranoid neobatrachians examined here had the LTPF tRNA gene cluster. Zhang et al. (2005a)

suggested that only a one-time gene rearrangement event caused the LTPF tRNA gene cluster in an ancestral lineage of neobatrachians. We also found the same tRNA gene cluster in three novel neobatrachian mtDNAs, supporting the hypothesis by Zhang et al. (2005a).

Phylogenetic analysis. For phylogenetic analyses, we used two datasets, amino acid and nucleotide data. The amino acid data contained 3,197 amino acid sites from 12 mt protein-encoding genes, and 1,574 sites were parsimoniously informative. The nucleotide data contained 10,974 nucleotide sites from 12 protein-encoding genes and 12S and 16S rRNA genes, and 6,346 sites were parsimoniously informative. Based on these data, the ML and BI analyses (with GTR+G+I model) reconstructed the same tree topology. Figure 7 shows the ML tree ($-\ln L = -67443.20$) obtained from the amino acid data. In this tree, amniotes and amphibians formed a monophyletic group. Among amphibians, our tree shows that each amphibian order (Anura, Urodela, and Caecilian) formed a clade, and Anura and Urodela became a monophyletic group. This topology supports the "batrachia hypothesis" (monophyly of Anura and Urodela among lissamphibians), as in the same case with previous phylogenetic studies based on mt genomic data (Zardoya and Meyer 2001). Although bootstrap supports of the Anura and Urodela clade were low (ML bootstrap = 69 and 58 for amino acid data and nucleotide data, respectively), Bayesian posterior probabilities (BPP) were high (100 for both amino acid and nucleotide data).

Within the anuran clade, archaeobatrachians and neobatrachians formed their own

clade with high statistical support (ML bootstrap and BPP = 100 for both amino acid and nucleotide data). The neobatrachian clade is recognized to include two major subgroups corresponding to the superfamilies Hyloidea and Ranoidea. In the hyloid clade, hylid and bufonid species formed monophyletic groups, respectively (ML bootstrap and BPP = 100 for both amino acid and nucleotide data). In the ranoid clade, the members of the family Microhylidae initially branched and the other group consisting of ranids, mantellids, and rhacophorids formed monophyletic groups (ML bootstrap and BPP = 100 for both amino acid and nucleotide data) corresponding to the epifamily Ranoidae. In this epifamily, the family Ranidae became a paraphyletic group with respect to Mantellidae and Rhacophoridae. In spite of the low BP values in our tree (ML bootstrap = 66 and 65, BPP = 99 and 100 for nucleotide and amino acid data, respectively), the paraphyletic nature of the family Ranidae has been supported by other systematic studies (Roelants et al., 2004; van der Meiden et al., 2005; Frost et al., 2006; Kurabayashi et al., 2006). Recently, Gissi et al. (2006) reported the complete mitochondrial sequences of two archaeobatrachian species, *Ascaphus truei* and *Pelobates cultripes*. We also carried out phylogenetic analyses including these taxa. The resultant BI tree based on amino acid data and ML tree based on all nuc data supported basal split of *Ascaphus* among anurans and sister relationship of *Pelobates* to the neobatrachian clade (Fig. 8), as well as recent molecular phylogeny studies using nuclear genes (Hoegg et al., 2004; Roelants and Bossyt, 2005; San Mauro et al., 2005). In contrast, the other analyses (ML based on amino acid, BI from all nuc, and BI and ML based on -3rd nuc data) support archaeobatrachian monophyly. Theses unstable

results are the same as the case of Gissi et al. (2006). These results seem to suggest that, even if some important archaeobatrachian data are added, mitochondrial genomic data are difficult to resolve archaeobatrachian relationships. Therefore, in the present study, we did not use these taxa in the following time estimation analyses.

Estimation of divergence times. We estimated divergence times among the amphibian taxa based on amino acid data of 12 H-strand-encoded protein genes [Fig. 9; many reference points not constrained as an absolute time (min-max values or min value) were recalculated by Multidivtime. Thus, some branching times used as reference points are also described.]. Tetrapoda separated from the common ancestor of Dipnoi in the Middle Devonian period at 393 Ma (407 – 378 Ma: 95% credibility interval) (node A in Fig. 9). The common ancestor of all amphibians separated from the other amniotes in the Early Carboniferous period at 355 (370 – 340) Ma (node B). In the amphibian clade, the divergence between Gymnophiona and Urodela + Anura occurred in the Middle Carboniferous period at 335 (352 – 317) Ma (node C), and the divergence between Urodela and Anura followed shortly thereafter in the Late Carboniferous period at 318 (337 – 298) Ma (node D).

The estimated divergence times of major tetrapod clades are similar to the estimated ages in a previous study using the mt genome (Zhang et al., 2005a). If we consider 95% confidence interval the most of our estimated times are also overlapped with those from San Mauro et al. (2005). Thus, the branching time inferences of these three studies are largely congruent. But the absolute time of each branching estimated in this study and

Zhang et al. (2005a) is slightly younger than San Mauro et al.'s estimations (Table 8). For example, the basal split between lissamphibians (node C in Fig. 9) at approx. 335 Ma was supported by the present study and Zhang et al. (2005a), while San Mauro et al. (2005) calculated it to be around 367 Ma. Lee and Anderson (2006) suggested that the discrepancy between the estimations of Zhang et al. and San Mauro et al. was caused by the different calibration methods they used: the former applied a single reference point, while the latter used multiple reference points. However, our analysis applied the same multiple reference points as San Mauro et al. (2005) and resulted in divergence times similar to those by Zhang et al. (2005a), indicating that the discrepancy was caused by the difference of molecular types used for analysis.

For the divergence times among anuran clades, the split between Archeobatrachia and Neobatrachia was estimated to be in the Late Carboniferous period at 297 (309 – 285) Ma (node E in Fig. 9). (As mentioned above, mitochondrial genomic data may not resolve the relationships of archaeobatrachian taxa with respect to neobatrachians and many of recent studies supported archaeobatrachian paraphyly. Thus, this branching time is only meaningful when the archaeobatrachian monophyly is true). Within the neobatrachian clade, Ranoidea and Hyloidea separated in Jurassic at 170 (186 – 154) Ma (node F), and subsequent divergences of neobatrachian families occurred from the Cretaceous to Tertiary periods. The split of Microhylidae and the epifamily Ranoidae occurred at 122 (107 – 137) Ma (node G), the basal split of *Fejervarya limonocharis* in the ranoid clade at 93 (81 – 105) Ma (node H), the split of Mantellidae + Rhacophoridae and family Ranidae at 83 (72 – 94) Ma (node I), Rhacophoridae and Mantellidae

separation at 73 (63 – 83) Ma (node J), and the split of Bufonidae and Hylidae at 97 (79 – 115) Ma (node K). These divergence times among anuran clades basically agree with those by Zhang et al. (2005a) (Table 8). However, neobatrachian branchings estimated from this study and Zhang et al. (2005a) were older than those by San Mauro et al. (2005). As for the split age of Ranoidea and Hyloidea (node F), our and Zhang et al.'s estimations (170 Ma and 172 Ma, respectively) closely matched another molecular time (approx. 170 Ma) estimated from the combined data of three mt and two nuclear genes (Vences et al., 2003). Furthermore, the branching time of Ranoidae and Microhylidae based on two mt and three nuclear genes (134 Ma; van der Meijden et al., 2005) is similar to our and Zhang et al.'s estimations (122 Ma and 142 Ma, respectively). For neobatrachian clades, therefore, our result seems to be closer to the majority opinion than San Mauro et al.'s estimation. The different estimations of the neobatrachian branchings between our (and Zhang et al's) study and San Mauro et al. may be caused by the fast evolutionary rate of mt genes among neobatrachian taxa. As discussed in the below section, substitution rate of mt gene is highly accelerated in neobatrachians and this fast rate seems to affect the older estimates of neobatrachian branchings.

With respect to some neobatrachian splits, our estimated values are slightly younger than those by Zhang et al. (2005a) (see table 8). For example, the branching time between the epifamily Ranoidae and Microhylidae was estimated to be 122 Ma in our analysis, while it was 142 Ma in Zhang et al. (2005a). This minor discrepancy might be due to the increased number of sampling taxa within neobatrachians (*B. buergeri, R. schlegelii, M. madagascariensis* and *F. limnocharis*) and multiple reference points

applied in this study. Zhang et al. (2005a) used limited taxa within neobatrachians (*R. nigromaculata, P. megacephalus, K. pulchra, M. heymonsi, B. melanostictus,* and *H. chinensis*) and no reference point within neobatrachians. The reference point within the neobatrachian clade (i.e. Mantellidae and Rhacophoridae split used here) seems to strongly affect molecular time dating (see the next section).

Based on amino acid data, the first split of neobatrachian families (i.e., Hyloidea and Ranoidea) was estimated within the Jurassic period corresponding to the early period of the breakup of Pangaea. Thus, our result seems to support the hypothesis that some ancestral lineages of modern neobatrachian families had already existed before the breakup of Pangaea, and were distributed over a wide range of this super continent (Roelants and Bossuyt, 2005; Zhang et al., 2005a; San Mauro et al., 2005). In addition, our analyses also showed the divergence times between the *Hyla*, *Bufo* and *Microhyla* species living in the Eurasian continent and in the Japanese archipelago. These branching periods and divergence times corresponded to the Tertiary period at 37 (58 – 17) Ma for *H. chinensis* and *H. japonica*, 43 (71 – 24) Ma for *B. melanostictus* and *B. japonicus,* and 37 (55 – 23) Ma for *M. heymonsi* and *M. okinavensis.* These are much earlier than the Late Miocene origin of Japanese *Bufo* species (about 6 Ma, Igawa et al., 2006), and thus suggest that the separations of Eurasian and Japanese frog taxa used here occurred in the ancient Eurasian continent before the Japanese archipelago formed. Furthermore, it is also remarkable that the divergence times of Eurasian – Japanese taxa in these families are similar (37 – 43 Ma). This might suggest that these branchings leading to Japanese frogs from other Eurasian lineages were caused by only a single

geographic event.

Assessing the quality of datasets and reference points. To investigate the influence of the data types on the divergence time estimation, we recalibrated the divergence times based on two other nucleotide datasets: all nuc (all nucleotides of 12 protein and rRNA genes) and –3rd nuc (nucleotides of 1st and 2nd codons of 12 protein genes and rRNA genes). Furthermore, to survey the reliability of the reference points, we also conducted the divergence time estimations with and/or without two specific reference points: between Mantellidae and Rhacophoridae (73.1 ± 19.5 Ma) (ref-set 2) and between diapsids and synapsids (310 ± 10 Ma) (ref-set 3). The former is the most recent reference point and the latter has been criticized due to the accuracy and precision of its age (Graur and Martin, 2004; Reisz and Müller, 2004a, b).

The resultant divergence times with all reference points (ref-set 1 in Fig. 9) showed that the times estimated based on both amino acid and –3rd nuc data were almost the same (Table 9). However, the times estimated with all nuc data showed somewhat older ages than the others at some nodes (G, J, H, and K) (Fig. 9 and Table 9), especially the divergences times among neobatrachians (J, H, and K). When the reference point between Mantellidae and Rhacophoridae was removed (ref-set 2), this older estimation was emphasized (Table 9). In contrast, for amino acid and –3rd nuc data, ref-sets 1 and 2 recovered similar estimated times (Table 9). Only 95% credibility ranges with ref-set 2 became slightly wider than those from ref-set 1. However, when the reference point between diapsids and synapsids was not applied (ref-set 3), the times estimated based

on all datasets showed slightly older times among early divergence of amphibians (node A, B, C, and D) than those calculated by using all reference points (ref-set 1) (Table 9).

To check the influence of substitution saturation on the time estimations, we plotted the uncorrected pairwise distances (= substitution rates) of each dataset against the estimated divergence times calculated from amino acid data (Fig. 9). According to the plots, the substitution rates among neobatrachians (solid circles in Fig. 9) are obviously faster than for the other taxa. This is considered to be because the tempo of substitution rates in the mt genome is extremely accelerated among neobatrachians, in agreement with the previous study (Hoegg et al., 2004). Furthermore, the substitution rate among neobatrachians showed the highest value at 93.3 Ma, for the comparisons between *F. limnocharis* and the other ranoids (shown as 'H' in Fig. 10), and the three following divergence points (96.6 Ma between Bufonidae and Hylidae; 122 Ma between Microhylidae and Ranidae; 170 Ma between Ranoidea and Hyloidea) showed lower nucleotide distances, indicating that a certain amount of saturation would have occurred among neobatrachian taxa. In Figs. 10A and B, however, the regression lines did not reach a plateau by the amino acid and –3rd nuc data. This indicates that substitutions were not saturated in these datasets. In contrast, all nuc data were highly saturated (Fig. 10C) in not only neobatrachians but also the other taxa, and the regression lines of the plotted points were almost parallel to the *x*-axis. Furthermore as shown in Fig. 10D, the saturation was mainly observed in codon 3rd positions of 12 protein genes.

These plot analyses suggest that the prior estimation from all codon sites (see above) was caused by the substitution saturation in this dataset. The saturated nucleotide sites

will underestimate the molecular distances (i.e., saturation will show fewer substitutions than actual substitutions), especially among deep branching taxa. Most of the reference points used here (excluding 73 Ma, Mantellidae and Rhacophoridae branching) correspond to possible saturated branches. If these deep branches are used as reference points, the prior assumption of substitution rate will be calculated slower than the actual rate. Although the Multidivtime program does not need to assume an equal rate molecular clock (Thorne et al., 1998), these erroneous prior assumptions would result in older branching times for other nodes especially shallow diverged taxa with less saturation (= having a larger actual number of substitutions). As shown in Fig. 10D, the codon 3rd positions were largely affected by substitution saturation. Thus, it is probable that the prior estimation from all nuc data was caused by substitution saturation in the codon 3rd positions. In addition, when we used ref-set 2, all nuc data showed even older times among neobatrachians. This suggests that the Mantellidae – Rhacophoridae split, the unique reference point within neobatrachians, is important to correct accelerated substitution rates in this taxon.

The amino acid and –3rd nuc data with less saturation resulted in similar and stable branching ages under ref-sets 1 and 2. Thus in these calibrations, Bayesian inference seems to efficiently correct the heterogeneity of substitution rate between taxa (i.e., archaeobatrachians and neobatrachians). However, the times estimated from these datasets become slightly older (at nodes B, C, D, and E, from amino acid data; node A, B, C, D, E, and F from –3rd nuc data) than those from the ref-set 3 without the calibration point between diapsids and synapsids. The diapsid-synapsid branching has

been used in many molecular time estimates, but several authors claimed the accuracy of this reference point based on paleontologic data (Graur and Martin, 2004; Reisz and Müller, 2004a, b). Our analyses showing a degree of instability estimated with and without this reference point suggest the ambiguity of this reference point.

Conclusion

In conclusion, for the divergence time estimation among amphibian taxa, it is considered that amino acid data resulted in fairly constant branching times, regardless of reference point setting. Furthermore, our results showed that the divergence times vary depending on both data types and selection of reference points. Although mitochondrial genes have been considered to be able to estimate accurate molecular distances even for ancient divergences (Kumazawa et al., 2004), nucleotide sequences of mitochondrial protein genes, especially codon 3rd positions, were rapidly saturated, and the saturated sites caused overestimated branching times for recently diverged taxa with less saturation. Furthermore, our results suggested that the application of multiple reference points was efficient to improve the accuracy of time estimations. Especially, the reference point between Mantellidae and Rhacophoridae seemed to be important to make an accurate estimate of branching time for neobatrachians. Because of the large heterogeneity of substitution rates between archaeobatrachian and neobatrachian mt genomes, it is important to increase other reference points within neobatrachians to improve the estimation of branching age for neobatrachians.

IV. General discussion

Phylogenetic relationships of *Bufo japonicus* subspecies group. To elucidate the evolutionary relationships of the *B. japonicus* subspecies group and closely related species, I conducted phylogenetic analyses based on seven mt genes. The resultant phylogeny showed that the *B. j. japonicus* subspecies group was divided into three major clades (Fig. 2A); i.e. the clade consisting of *B. j. gargarizans, B. j. bankorensis,* and *B. j. miyakonis*, and the two clades consisting of western and eastern *B. j japonicus.* Within these eastern and western groups, the subclades well matched with their geographic distribution patterns. These relationships also agreed with the previous studies: morphology (Inger, 1972), karyology (Matsui, 1980), allozyme analysis (Nishioka et al., 1990; Kawamura et al., 1990), and crossing experiments (Kawamura et al., 1980, 1982).

Divergence times and inferred biogeographic events causing divergences of *Bufo japonicus* subspecies. On the basis of divergence times estimated here, I inferred the biogeographic events that caused the major branchings of the *Bufo* species groups. Initial branching between Eurasian continental and Japanese toads was estimated to have occurred in the Late Miocene (approx. 6.8 Ma; Fig. 2B, clade 2). The Japanese *Bufo* species diverged into two major groups (eastern and western) in the Early Pliocene at (approx. 5.7 Ma, Fig 2B, clade 3)

These estimated divergence times are almost the same with the era when the two

massive geographic events occurred. The first is the resuming of Philippine Sea plate (PHS) subduction in the Late Miocene, (Fig. 4C) (Kamata, 1999; Kamata and Kodama, 1994; Itoh and Nagasaki, 1996). The second is the expansion of many basins at an intra-arc depressional zone called the Setouchi Geologic Province and the back arc area of a mainland known as the Green Tuff region in the Early Pliocene (Fig. 4D) (Itoigawa, 1991; Yoshida, 1992; Kuwahara, 1985). The first event might have broken the land bridge from the Korean Peninsula to the Japanese Archipelago and caused the isolation of the ancient Japanese *Bufo* species from continental species. The second event might have segmented the distribution area of ancestral Japanese *Bufo* species. In addition, the uplifting and volcanic activity occurred in this area after the second event, which transformed the neighboring landmass in the Pliocene (Takeuchi, 1999a, b). The mountains, basins, and other geographic features in this area might have restricted dispersal of *B. j. torrenticola* from this mountainous area, thereby isolating this subspecies and setting the stage for morphological differentiation.

On the other hand, the divergence among *B. j. miyakonis, B. j. gargarizans* and *B. j. bankorensis* was estimated to have occurred in the Pleistocene era approx. 1 Ma. The oldest fossil record of *B. j. miyakonis* from the Late Pleistocene (< 1 Ma) deposited on Miyako Island (Nokariya and Hasegawa, 1985) seems to agree with my result. Furthermore, no native populations or fossil records of the genus *Bufo* have ever been found in the other Ryukyu Islands (Ota, 2003). A similar distribution pattern and divergence have also been reported for the lizard *Takydromus toyamai* (Ota et al., 2002) and snakes *Amphiesma concelarum* and *Calamaria pfefferi* (Ota, 1998). Therefore, the

estimated divergence times of *Bufo* and the distribution patterns of animals seem to support the hypothesis that the disjunction between Miyako Island and the other Ryukyu Islands (approx. 6 Ma, Late Miocene) preceded the fragmentation of Miyako Island and the Eurasia continent/Taiwan (approx. 1 Ma; Ota, 1998).

In conclusion, I showed that the branching dates of *Bufo japonicus* subspecies estimated from mtDNA data matched with the ancient geographic events of the Eurasian continent and Japanese Archipelago, and these events might be the causes of divergences of *Bufo japonicus* subspecies.

Divergence times between continental and Japanese species based on mt genomic data.

To estimate the divergence times of continental and Japanese frog species including *Bufo* species, I also conducted the divergence time estimation in the higher taxonomic level based on a large molecular dataset (12 mitochondrial protein genes; Fig. 9). As a result, the divergence times between the *Hyla*, *Bufo* and *Microhyla* species living in the Eurasian continent and in the Japanese archipelago were estimated in the Tertiary period. These were much earlier than the Late Miocene origin of Japanese *Bufo* species (about 6 Ma); and thus, it was suggested that the separations of Eurasian and Japanese frog taxa used here occurred in the ancient Eurasian continent before the formation of Japanese archipelago. Furthermore, it is also remarkable that the divergence times of Eurasian – Japanese taxa in these different frog families were very similar (37 – 43 Ma). This might suggest that these branchings leading to Japanese frogs from other Eurasian lineages were caused by single geographic event.

Mitochondrial genome composition of three neobatrachian frogs. I determined the complete mt genomes of three neobatrachian frogs (*B. japonicus, H. japonica,* and *M. okinavensis*). These mt genomes commonly encoded 37 typical mt genes (i.e., 13 protein, two rRNA, and 22 tRNA genes), and all of these genes were similar in length to their counterparts in other anurans. Contrary to this, the genome sizes of these three mtDNAs highly diverged, ranging from 16,717 (*M. okinavensis*) to 19,519 bp (*H. japonica*) (Table 6). These differences were caused by length differences in their control regions (Fig. 6). In *B. japonicus* and *H. japonica* mtDNAs, the control regions possessed two tandem repeats at both 5' and 3' ends, and these repeats made long control regions (2,351 bp and 4,103 bp, respectively). In contrast, the control region of *M. okinavensis* did not include repeat units and its length was 1,335 bp (Fig. 6).

The structures of the control regions among closely related species, most features were shared within the same genus (Fig. 6). For *Bufo* and *Hyla* species, the control regions of these species commonly possessed repeat motifs at both 5' and 3' ends. On the other hand, no obvious repeat motifs were found in the control region of microhylids, which is the chief factor responsible for the relatively short control region. Microhylid control regions without any repeat motif are unusual, because almost all anuran control regions contain several repeat motifs, particularly, in most reported mtDNAs from superfamily Ranoidae: *Rana nigromaculata* (Sumida et al., 2001), *Buergeria buergeri* (Sano et al., 2004), *Rhacophorus schlegelii* (Sano et al., 2005), and *Mantella madagascariensis* (Kurabayashi et al., 2006). Therefore, the microhylid control regions

lacking repeat sequences seem to be a synapomorphy originating in a common ancestor of this family.

Phylogenetic relationship of major among anuran clades. Based on the mt genomic data, I reconstructed phylogenetic tree among anurans. In the resultant tree (Fig. 7), Anura and Urodela formed a monophyletic group, supporting "batrachia hypothesis", as in the same case with the previous phylogenetic studies based on mt genomic data (Zardoya and Mayer 2001). Within the anuran clade, archaeobatrachians and neobatrachians formed their own clade with high statistical supports. In the neobatrachian clade, two major subgroups corresponding to the superfamilies Hyloidea and Ranoidea were recognized. In the ranoid clade, the members of the family Microhylidae initially branched and the other group, ranids, mantellids, and rhacophorids, formed a monophyletic group corresponding to the epifamily Ranoidae. In this epifamily, the family Ranidae became a paraphyletic group with respect to Mantellidae and Rhacophoridae. The paraphyletic nature of the family Ranidae has been supported by other systematic studies (Roelants et al., 2004; van der Meiden et al., 2005; Frost et al., 2006; Kurabayashi et al., 2006).

Estimation of divergence times among anurans. The divergence times of major tetrapod clades estimated here are similar to these suggested by the previous study using the mt genome data (Zhang et al., 2005a) (Table 8). However, neobatrachian branchings estimated by this study and Zhang et al. (2005a) were older than those from nuclear

gene data by San Mauro et al. (2005). The different estimations of the neobatrachian branchings between the present (and Zhang et al's) studies and San Mauro et al.'s ones may be caused by the fast evolutionary rate of mt genes among neobatrachian taxa (see blow)

With respect to some neobatrachian splits, the values estimated in this study are slightly younger than those by Zhang et al. (2005a) This minor discrepancy might be due to the increased number of sampling taxa within neobatrachians and multiple reference points applied in this study. Zhang et al. (2005a) used limited taxa within neobatrachians and no reference point within neobatrachians. The reference point within the neobatrachian clade used here (i.e. Mantellidae and Rhacophoridae split) seems to strongly affect molecular time dating.

The first split of neobatrachian families (i.e., Hyloidea and Ranoidea) was estimated within the Jurassic period corresponding to the early period of the breakup of Pangaea. Thus, my result seems to support the hypothesis that some ancestral lineages of modern neobatrachian families had already existed before the breakup of Pangaea, and were distributed over a wide range of continents which are descendant of this super continent (Roelants and Bossuyt, 2005; Zhang et al., 2005a; San Mauro et al., 2005).

To investigate the influence of the data types and calibration point settings on the divergence time estimation, I recalibrated the divergence times based on two other nucleotide datasets and two specific reference points. As the result of the divergence time estimation among amphibian taxa, it is considered that amino acid data resulted in fairly constant branching times, regardless of reference point setting. Furthermore, I showed that the

divergence times varied depending on both data types and selection of reference points. Although mitochondrial genes have been considered to be able to estimate accurate molecular distances even for ancient divergences (Kumazawa et al., 2004), substitutions of mitochondrial protein genes, especially 3rd codon positions, were rapidly saturated, and the saturated sites caused overestimated branching times for recently diverged taxa with less saturation. Furthermore, my results suggested that the application of multiple reference points was efficient to improve the accuracy of time estimations. Especially, the reference point between Mantellidae and Rhacophoridae seemed to be important to make an accurate estimate of branching time for neobatrachians. Because of the large heterogeneity of substitution rates between archaeobatrachian and neobatrachian mt genomes, it is important to increase other reference points within neobatrachians in order to improve the estimation of branching age for neobatrachians.

Acknowledgments

I express my sincere thanks o Professor M. Sumida, and Dr. A. Kurabayashi, Hiroshima University, for their invaluable advice, discussion and encouragement throughout the course of this study. I am indebted to Dr. H. Yamasaki, Hiroshima University, and Professor H. Ota, University of Ryukyus, for helpful comments and suggestions on geology and biogeography, Professor Chih-Ye Chang, Institute of Zoology, Academica Sinica, Mr. C. S. Wang and Mr. P. S. Lin, National Taiwan University, Dr. E. Crespo, Museu e Laboratorio, Zoologico e Antropologica, Faculdade de Ciencias-Universidade, Portugal, Professor T. Otsu, Yamagata University, Dr. N. Shinozaki, Amphibian Laboratory of Nikko, Professor M. Tadano, Gifu University, Professor S. Ishikubo, Kagoshima University, Professor M. Kuramoto, Fukuoka Educational University, Professor M. Matsui, Kyoto University, Mr. R. Shimoyama, Nagano Prefecture, Mr. M. Sakuyama, Hakodate City, Mr. S. Okada, Shimane University, and Mr. Y. Yuasa, Hyogo Prefecture for collecting and providing valuable specimens. Thanks are also due to Dr. A. Kanda, Dr. N. Sano, Mr. J. Satoh, Mr. T. Yamamoto, and all members of Sumida laboratory, for their advice and encouragement.

References

Abascal, F., Zardoya, R., and Posada, D. (2005) ProtTest: selection of best-fit models of protein evolution. Bioinformatics **21**, 2104-2105.

Adachi, J., and Hasegawa, M. (1996) Model of amino acid substitution in proteins encoded by mitochondrial DNA. J. Mol. Evol. **42**, 459-468.

Amer, S. A. M., and Kumazawa, Y. (2005) Mitochondrial genome of *Pogona vitticepes* (Reptilia; Agamidae): control region duplication and the origin of Australasian agamids. Gene **346**, 249-256.

Anderson, S., Bankier A. T., Barrell, B. G., de Bruijn, M. H. L., Coulson, A. R., Drouin, J., Eperon, I. C., Nierlich, D. P., Roe, B. A., Sanger, F., Schreier, P. H., Smith, A. J. H., Staden, R., and Young, I. G. (1981) Sequence and organization of the human mitochondrial genome. Nature **290**, 457-465.

Atsumi, S., Ohta, S., and Sumida, M. (1998) Sex differences in polymorphism and expression of AAT-1 in the Hiroshima population of *Buergeria buergeri* (Anura, Rhacophoridae). Zool. Sci. **15**, 469-475.

Avise, J. C. (1994) Molecular Markers, Natural History and Evolution. Chapman & Hall, New York.

Baez, A. M. (2000) Tertiary anurans from South America. In: Amphibian biology. (Eds.: H. Heatwole, and R. L. Carroll), pp. 1388-1401. Surrey Beatty, Chipping Norton, Australia.

Benton, M. J. (1990) Phylogeny of the major tetrapod groups: morphological data and divergence dates. J. Mol. Evol. **30**, 409-924.

Boore, J. L. (1999) Survey and Summary: Animal mitochondrial genomes. Nucleic Acid Res. **27**, 1767-1780.

Bossuyt, F., and Milinkovitch, M. (2001) Amphibians as indicators of early tertiary "out-of-India" dispersal of vertebrates. Science **292**, 93-95.

Castresana, J. (2000) Selection of conserved blocks from multiple alignments for their use in phylogenetic analysis. Mol. Biol. Evol. **17**, 540-552.

Dunon-Bluteau, D., and Brun, G. (1986) The secondary structures of the *Xenopus laevis* and human mitochondrial small ribosomal subunit RNA are similar. FEBS Lett. **198**, 333-338.

Farris, J. S., Kallersjo, M., Kluge, A. G., and Bult, C. (1995) Constructing a significance test for incongruence. Syst. Biol. **44**, 570-672.

Frost, D. R. et al. (2006) The amphibian tree of life. Bull. Amer. Mus. Nat. Hist. **297**, 1-291.

Gao, K. Q., and Shubin, N. H. (2001) Late Jurassic salamanders from northern China. Nature **410**, 574-577.

Gissi, C., San Mauro, D., Pesole, G., and Zardoya, R. (2006) Mitochondrial phylogeny of Anura (Amphibia): A case study of congruent phylogenetic reconstruction using amino acid and nucleotide characters. Gene **366**, 228-237.

Graur, D., and Martin, W. (2004) Reading the entrails of chickens: molecular timescales of evolution and the illusion of precision. Trends Genet. **20**, 80-86.

Guindon, S., and Gascuel, O. (2003) A simple, fast, and accurate algorithm to estimate large phylogenies by maximum likelihood. Syst. Biol. **52**, 696-704.

Harrison, T. M., Copeland, P., Kidd, W. S. F., and Yin, A. (1992) Raising Tibet. Science **255**, 1663-1670.

Hayashi, T., and Matsui, M. (1988) Biochemical differentiation in Japanese newts, genus *Cynops* (Salamandridae). Zool. Sci. **5**, 1121-1136.

Henikoff, S. (1987) Exonuclease Ⅲ generated deletions for DNA sequence analysis. Promega Notes No. 8.

Hikida, T., Ota, H., Kuramoto, M., and Toyama, M. (1989) Zoogeography of Amphibians and Reptiles in East Asia. Curr. Herpetol. in East Asia 278-281.

Hoegg, S., Vences, M., Brinkmann, H., and Meyer, A. (2004) Phylogeny and comparative substitution rates of frogs inferred from sequences of three nuclear genes. Mol. Biol. Evol. **21**, 1188-1200.

Huelsenbeck, J. P., and Ronquist, F. (2001) MRBAYES: Bayesian inference of phylogenetic trees. Bioinformatics **17**, 754-775.

Igawa, T., Kurabayashi, A., Nishioka, M., and Sumida, M. (2006) Molecular phylogenetic relationship of toads distributed in the Far East and Europe inferred from the nucleotide sequences of mitochondrial DNA genes. Mol. Phylogenet. Evol. **38**, 250-260.

Inger, R. F. (1972) *Bufo* of Eurasia. In: Evolution in the Genus *Bufo*. (Ed.: W. F. Blair), pp. 102-118. Univ. Texas Press, Austin, Texas

Ito, Y., and Nagasaki, Y. (1996) Crustal shortening of Southwest Japan in the Late Miocene. Isl. Arc. **5**, 337-353.

Itoigawa, J. (1991) Miocene sedimentary basins and molluscan faunas in Southwest

Japan. Saito Ho-on Kai Spec. Pub. 295-302.

Kamata, H., and Komada, K. (1989) Volcanic history and tectonics of the Southwest Japan Arc. Isl. Arc. **8**, 393-403.

Kamata, H., and Kodama, K. (1994) Tectonics of an arc-arc junction: an example from Kyushu Island at the junction of the Southwest Japan Arc and the Ryukyu Arc. Tectonophysics **233**, 69-81.

Kamata, H. (1999) The importance of the broad tectonic changes at the junction of the Southwest Japan Arc and the Ryukyu Arc at 6Ma and 2Ma. Chikyu Mon. **21**, 630-636. [In Japanese]

Kawamura, T., Nishioka, M., and Ueda, H. (1980) Inter- and intraspecific hybrids among Japanese, European and American toads. Sci. Rep. Lab. Amphib. Biol. Hiroshima Univ. **4**, 1-125.

Kawamura, T., Nishioka, M., kondo, Y., and Wu, Z. (1982) Viability of hybrids among Japanese, Taiwan, European and American toads. Jpn. J. Genet. **57**, 677-678. [In Japanese]

Kawamura, T., Nishioka, M., Sumida, M., and Ryuzaki, M. (1990) An electrophoretic study of genetic differentiation in 40 populations of *Bufo japonicus* distributed in Japan. Sci. Rep. Lab. Amphib. Biol. Hiroshima Univ. **10**, 1-51.

Kishino, H., and Hasegawa, M. (1989) Evaluation of the maximum likelihood estimate of the evolutionary tree topologies from DNA sequence data, and the branching order in Hominoidea. J. Mol. Evol. **29**, 170-179.

Kishino, H., Thorne, J. L., and Bruno, W. J. (2001) Performance of a divergence time

estimation method under a probabilistic model of rate evolution. Mol. Biol. Evol. **18**, 352-361.

Kizaki, K., and Oshiro, I. (1980) The origin of the Ryukyu Islands. In: Natural History of the Ryukyus. (Ed.: K. Kizaki), pp. 8-37. Tsukiji-Shokan, Tokyo, Japan. [In Japanese]

Kocher, T. D., and Stepien, C. A. (1997) Molecular systematics of fishes. Academic Press, New York.

Kraft, R., Tardiff, J., Krauter, K., and Leinwand, L. (1988) Using mini-prep plasmid DNA for sequencing double stranded templates with Sequenase. Biotechniques **6**, 544-549.

Kumar, S., and Hedges, S. B. (1998) A molecular timescale for vertebrate evolution. Nature **392**, 917-920.

Kumar, S., Tamura, K., Jakobsen, I., and Nei, M. (2001) MEGA2: molecular evolutionary genetics analysis software. Bioinformatics **17**, 1244-1245.

Kumazawa, Y., Azuma, Y., and Nishida, M. (2004) Tempo of mitochondrial gene evolution: Can mitochondrial DNA be used to date old divergences? Endocytobiosis Cell Res. **15**, 136-142.

Kurabayashi, A., Usuki, C., Mikami, N., Fujii, T., Yonekawa, H., Sumida, M., and Hasegawa, M. (2006) Complete nucleotide sequence of the mitochondrial genome of a Malagasy poison frog *Mantella madagascariensis*: evolutionary implications on mitochondrial genomes of higher anuran groups. Mol. Phylogenet. Evol. **39**, 223-236.

Kuwahara, T. (1985) Characteristics of the tectonic movement in the Setouchi province. Chidanken Senpo **29**, 171-189. [In Japanese]

Lee, M. S. Y., and Anderson, J. S. (2006) Molecular clocks and the origin(s) of modern amphibians. Mol. Phylogenet. Evol. **40**, 635-639.

Liu, Z., Wang, Y., and Su, B. (2005) The mitochondrial genome organization of the rice frog, *Fejervarya limnocharis* (Amphibia: Anura): a new gene order in the vertebrate mtDNA. Gene **346**, 145-151.

Nishioka, M., Sumida, M., Ueda, H., and Wu, Z. (1990) Genetic relationshops among 13 *Bufo* species and subspecies elucidated by the method of electrophoretic analyses. Sci. Rep. Lab. Amphib. Biol. Hiroshima Univ. **10**, 53-91.

Nishioka, M., Kodama, Y., Sumida, M., and Ryuzaki, M. (1993) Systematic evolution of 40 populations of *Rana rugosa* distributed in Japan elucidated by electrophoresis. Sci. Rep. Lab. Amphib. Biol. Hiroshima Univ. **12**, 83-131.

Nokariya, H., and Hasegawa, Y. (1985) Fossil frogs from Pinza-Abu Cave. Miyako Island, Okinawa, Japan. In: Reports on Excavation of the Pinza-Abu Cave. pp. 151-159. Okinawa Prefectural Board of Education, Naha. [In Japanese]

Macey, J., Schulte, J., Larson, A., Fang, Z., Wang, Y., Tuniyev, B., and Papenfuss, T. (1998) Phylogenetic relationships of toads in the *Bufo bufo* species group from the eastern escarpment of the Tibetan Plateau: a case of vicariance and dispersal. Mol. Phylogenet. Evol. **9**, 80-87.

Matsui, M. (1976) A new toad from Japan. Contr. Biol. Lab. Kyoto Univ. **25**, 1-9.

Matsui, M. (1980) Karyology of Eurasian toads of the *Bufo bufo* complex. Annot. Zool.

Jpn. **53**, 56-68.

Matsui, M. (1984) Morphometric variation analyses and revision of the Japanese toads (Genus *Bufo*, Bufonidae). Contr. Biol. Lab. Kyoto Univ. **26**, 209-428.

Milner, A. R. (1993) Amphibian-Grade Tetrapoda. In: The Fossil Record 2. (Ed.: M. J Benton), pp. 665-679. Chapman and Hall, London.

Mueller, R. L., and Boore, J. L. (2005) Molecular mechanisms of extensive mitochondrial gene rearrangement in plethodontid salamanders. Mol. Biol. Evol. **22**, 2104-2112.

Mulcahy, D. G., and Mendelson, J. R., III (2000) Phylogeography and speciation of the morphologically variable, widespread species Bufo valliceps, based on molecular evidence from mtDNA. Mol. Phylogenet. Evol. **17**, 173-189.

Ota, H. (1998) Geographic patterns of endemism and speciation in amphibians and reptiles of the Ryukyu Archipelago, Japan, with special reference to their palaeogeographical implications. Res. Popul. Ecol. **40**, 189-204.

Ota, H., Honda, M., Chen, S., Hikida, T., Panha, S., Oh, H., and Matsui, M. (2002) Phylogenetic relationships, taxonomy, character evolution and biogeography of the lacertid lizards of the genus *Takydromus* (Reptilia: Squamata): a molecular perspective. Biol. J. Linn. Soc. Lond. **76**, 493-509.

Ota, H. (2003) Toward a synthesis of paleontological and neontological information on the terrestrial vertebrates of the Ryukyu archipelago. I. Systematic and biogeographic review. J. Fossil Res. **36**, 43-59.

Pitman, W.C., III, Cande, S., LaBrecque, J., and Pindell, J. (1993) Fragmentation of

Gondwana: the separation of Africa from South America. In: Biological relationships between Africa and South America. (Ed.: P. Goldblatt), pp. 15-34. Yale University Press, New Haven, Connecticut.

Posada, D., and Crandall, K. (1998) MODELTEST: testing the model of DNA substitution. Bioinformatics **14**, 817-818.

Rage, J., and Rocek, Z. (1989) Redescription of *Triadobatrachus massinoti* (Piveteau, 1936) and anuran amphibian from the early Triassic. Palaeontographica Abt. A. **206**, 1-16.

Reisz, R. R., and Müller, J. (2004a) Molecular timescales and the fossil record: a paleontological perspective. Trends Genet. **20**, 237-241.

Reisz, R. R., and Müller, J. (2004b) The comparative method for evaluating fossil calibration dates: a reply to Hedges and Kumar. Trends Genet. **20**, 596-597.

Rocek, Z. (2000) Mesozoic anurans. In: Amphibian biology (Eds.: H. Heatwole, and R. L. Carroll), pp.1295-1331. Surrey Beatty, Chipping Norton, Australia.

Rodriguez, F., Oliver, J. F., Marin, A., and Medina, J. R. (1990) The general stochastic model of nucleotide substitution. J. Theor. Biol. **142**, 485-501.

Roe, B. A., Ma, D. P., Wilson, R. K., and Wong, J. F. H. (1985) The complete nucleotide sequence of the *Xenopus laevis* mitochondrial genome. J. Biol. Chem. **260**, 9759-9774.

Roelants, K., and Bossuyt, F. (2005) Archaeobatrachian paraphyly and pangaean diversification of crown-group frogs. Syst. Biol. **54**, 111-126.

Roelants, K., Gower, D. J., Wilkinson, M., Loader, S. P., Biju, S. D., Guillaume, K.,

Moriau, L., and Bossuyt, F. (2007) Global patterns of diversification in the history of modern amphibians. Proc. Natl. Acad. Sci. U S A **104**, 887-892.

Roelants, K., Jiang, J., and Bossuyt, F. (2004) Endemic ranid (Amphibia: Anura) genera in southern mountain ranges of the Indian subcontinent represent ancient frog lineages: evidence from molecular data. Mol. Phylogenet. Evol. **31**, 730-740.

Sambrook, J., and Russell, D. W. (2001) Molecular Cloning: A Laboratory Manual, third ed. Cold Spring Harbor Laboratory Press, Cold Spring Harbor, New York.

San Mauro, D., García-París, M., and Zardoya, R. (2004) Phylogenetic relationships of discoglossid frogs (Amphibia: Anura: Discoglossidae) based on complete mitochondrial genomes and nuclear genes. Gene **343**, 357-366.

San Mauro, D., Vences, M., Alcobendas, M., Zardoya, R., and Meyer, A. (2005) Initial diversification of living amphibians predated the breakup of Pangaea. Am. Nat. **165**, 590-599.

San Mauro, D., Gower, D. J., Zardoya, R., and Wilkinson, M. (2006) A hotspot of gene order rearrangement by tandem duplication and random loss in the vertebrate mitochondrial genome. Mol. Biol. Evol. **23**, 227-234.

Sano, N., Kurabayashi, A., Fujii, T., Yonekawa, H., and Sumida, M. (2004) Complete nucleotide sequence and gene rearrangement of the mitochondrial genome of the bell-ring frog, *Buergeria buergeri* (family Rhacophoridae). Genes Genet. Syst. **79**, 151-163.

Sano, N., Kurabayashi, A., Fujii, T., Yonekawa, H., and Sumida, M. (2005) Complete nucleotide sequence of the mitochondrial genome of Schlegel's tree frog

Rhacophorus schlegel (family Rhacophoridae): duplicated control regions and gene rearrangements. Genes Genet. Syst. **80**, 213-224.

Sbisà, E., Tanzariello, F., Reyes, A., Pesole, G, and Saccone, C. (1997) Mammalian mitochondrial D-loop region structural analysis: identification of new conserved sequences and their functional and evolutionary implications. Gene **205**,125-140.

Seddon, J. M., Baverstock, P. R., Georges, A. (1998) The rate of mitochondrial 12S rRNA gene evolution is similar in freshwater turtles and marsupials. J. Mol. Evol. **46**, 460-464.

Shimodaira, H., and Hasegawa, M. (1999) Multiple comparison of log-likelihoods with applications to phylogenetic inference. Mol. Biol. Evol. **16,** 1114-1116.

Sumida, M., Kanamori, Y., Kaneda, H., Kato, Y., Nishioka, M., Hasegawa, M., and Yonekawa, H. (2001) Complete nucleotide sequence and gene rearrangement of the mitochondrial genome of the Japanese pond frog *Rana nigromaculata.* Genes Genet. Syst. **76**, 311-325.

Sumida, M., Ogata, M., and Nishioka, M. (2000) Molecular phylogenetic relationships of pond frogs distributed in the Palearctic region inferred from DNA sequences of mitochondrial 12S ribosomal RNA and cytochrome b genes. Mol. Phylogenet. Evol. **16**, 278-285.

Sumida, M., Ohta, S., Atsumi, S., and Fujii, T. (2004) Geographic variability in expression of the sex-linked AAT-1 gene of the bell-ring frog, *Buergeria buergeri.* J. Exp. Zoolog. Part. B Mol. Dev. Evol. **302**, 182-194.

Swofford, D. L. (2003) PAUP*. Phylogenetic Analysis Using Parsimony (*and Other

Methods). Version 4. Sinauer Associates, Sunderland, MA.

Tajima, F. (1993) Simple methods for testing molecular clock hypothesis. Genetics **135**, 599-607.

Takehana, Y., Nagai N., Matsuda M., Tsuchiya K., and Sakaizumi M. (2003) Geographic variation and diversity of the Cytochirome *b* gene in Japanese wild populations of Medaka, *Oryzias latipes*. Zool. Sci. **20**, 1279-1291.

Takeuchi, A. (1999a) Neotectonics and tectonic region in Japanese Archipelago. Chikyu Mon. **21**, 537-542. [In Japanese]

Takeuchi, A. (1999b) Changes of stress field and tectonics scince Pliocene at the Hokushinetsu district. Chikyu Mon. **21**, 583-588. [In Japanese]

Thompson, J. D., Higgins, D. G., and Gibson, T. J. (1994) CLUSTAL W: improving the sensitivity of progressive multiple sequence alignment through sequence weighting, position-specific gap penalties and weight matrix choice. Nucleic Acids Res, **22**, 4673-4680.

Thompson, J. D., Gibson, T. J., Plewniak, F., Jeanmougin, F., and Higgins, D. G. (1997) The CLUSTAL_X windows interface: flexible strategies for multiple sequence alignment aided by quality analysis tools. Nucleic. Acids Res. **25**, 4876-4882.

Thorne, J. L., and Kishino, H. (2002) Divergence time and evolutionary rate estimation with multilocus data. Syst. Biol. **51**, 689-702.

Thorne, J. L., Kishino, H., and Painter, I. S. (1998) Estimating the rate of evolution of the rate of molecular evolution. Mol. Biol. Evol. **15**, 1647-1657.

Tzeng, C. S., Hui, C. F., Shen, S. C., and Huang, P. C. (1992) The complete nucleotide

sequence of the *Crossostoma lacustre* mitochondrial genome: conservation and variations among vertebrates. Nucleic Acids Res. **20**, 4853-4858.

van der Meijden, A., Vences, M., Hoegg, S., and Meyer, A. (2005) A previously unrecognized radiation of ranid frogs in Southern Africa revealed by nuclear and mitochondrial DNA sequences. Mol. Phylogenet. Evol. **37**, 674-685.

Vences, M., Vieites, D. R., Glaw, F., Brinkmann, H., Kosuch, J., Veith, M., and Meyer, A. (2003) Multiple overseas dispersal in amphibians. Proc. R. Soc. Lond. B Biol. Sci. **270**, 2435-2442.

Wilgenbusch J. C., Warren D.L., and Swofford D.L. (2004) AWTY: A system for graphical exploration of MCMC convergence in Bayesian phylogenetic inference. http://ceb.csit.fsu.edu/awty.

Wolstenholme, D. R. (1992) Animal mitochondrial DNA: structure and evolution. In: Mitochondrial genomes. (Eds.: D. R. Wolstenholme, and K. W. Jeon), pp. 173-216. Academic Press, New York.

Yang, Z. (1997) PAML: a program package for phylogenetic analysis by maximum likelihood. Comput. Appl. Biosci. **13**, 555-556.

Yoshida, F. (1992) Geologic development of the Setouchi Geologic Province since Early Miocene - with special reference to the First and Second Setouchi Inland Sea times. Bull. Geol. Surv. Japan. **43**, 43-67. [In Japanese]

Zardoya, R., and Meyer, A. (2001) On the origin of and phylogenetic relationships among living amphibians. Proc. Natl. Acad. Sci. U S A **98**, 7380-7383.

Zhang, P., Zhou, H., Chen, Y. Q., Liu, Y. F., and Qu, L. H. (2005a) Mitogenomic

perspectives on the origin and phylogeny of living amphibians. Syst. Biol. **54**, 391-400.

Zhang, P., Zhou, H., Liang, D., Liu, Y .F., Chen, Y. Q., and Qu, L. H. (2005b) The complete mitochondrial genome of a tree frog, *Polypedates megacephalus* (Amphibia: Anura: Rhacophoridae), and a novel gene organization in living amphibians. Gene **346**, 133-143.

Tables & Figures

Table 1. Specimens used and haplotypes of nucleotide sequences of the mitochondrial DNA genes.

Species	Collecting station		Abbreviation	Accession Nos.		
	Country	Locality, Prefecture		Cyt *b*	tRNAs and 12S rRNA	16S rRNA
1. *Bufo japonicus japonicus*	Japan	Hakodate, Hokkaido	B.j.jap. (Hakodate)	AB159232	AB159448	AB159561
2. *Bufo japonicus japonicus*	Japan	Hirosaki, Aomori	B.j.jap. (Hirosaki)	AB159233	AB159449	AB159562
3. *Bufo japonicus japonicus*	Japan	Mt. Iwaki, Aomori	B.j.jap. (Iwaki)	AB159234	AB159450	AB159563
4. *Bufo japonicus japonicus*	Japan	Wakuya, Miyagi	B.j.jap. (Wakuya)	AB159235	AB159451	AB159564
5. *Bufo japonicus japonicus*	Japan	Atsumi, Yamagata	B.j.jap. (Atsumi)	AB159236	AB159452	AB159565
6. *Bufo japonicus montanus*	Japan	Zao, Yamagata	B.j.mon. (Zao)	AB159237	AB159453	AB159566
7. *Bufo japonicus montanus*	Japan	Nikko, Tochigi	B.j.mon. (Nikko)	AB159238	AB159454	AB159567
8. *Bufo japonicus japonicus*	Japan	Kuji, Ibaraki	B.j.jap. (Kuji)	AB159239	AB159455	AB159568
9. *Bufo japonicus japonicus*	Japan	Kashiwa, Chiba	B.j.jap. (Kashiwa)	AB159240	AB159456	AB159569
10. *Bufo japonicus japonicus*	Japan	Agatsuma, Gunma	B.j.jap. (Azuma)	AB159241	AB159457	AB159570
11. *Bufo japonicus japonicus*	Japan	Tone, Gunma	B.j.jap. (Tone)	AB159242	AB159458	AB159571
12. *Bufo japonicus japonicus*	Japan	Chichibu, Saitama	B.j.jap. (Chichibu)	AB159243	AB159459	AB159572
13. *Bufo japonicus japonicus*	Japan	Zama, Kanagawa	B.j.jap. (Zama)	AB159244	AB159460	AB159573
14. *Bufo japonicus japonicus*	Japan	Suwa, Nagano	B.j.jap. (Suwa)	AB159245	AB159461	AB159574
15. *Bufo japonicus japonicus*	Japan	Hamamatsu, Shizuoka	B.j.jap. (Hamamatsu)	AB159246	AB159462	AB159575
16. *Bufo japonicus japonicus*	Japan	Neo, Gifu	B.j.jap. (Neo)	AB159247	AB159463	AB159576
17. *Bufo japonicus torrenticola*	Japan	Neo, Gifu	B.j.tor. (Neo)	AB159248	AB159464	AB159577
18. *Bufo japonicus torrenticola*	Japan	Odai, Nara	B.j.tor. (Odai)	AB159249	AB159465	AB159578
19. *Bufo japonicus japonicus*	Japan	Arashiyama, Kyoto	B.j.jap. (Arashi)	AB159250	AB159466	AB159579
20. *Bufo japonicus japonicus*	Japan	Kodera, Hyogo	B.j.jap. (Kodera)	AB159251	AB159467	AB159580
21. *Bufo japonicus japonicus*	Japan	Nichinan, Tottori	B.j.jap. (Nichinan)	AB159252	AB159468	AB159581
22. *Bufo japonicus japonicus*	Japan	Yoshiwa, Hiroshima	B.j.jap. (Yoshiwa)	AB159253	AB159469	AB159582
23. *Bufo japonicus japonicus*	Japan	Hiroshima, Hiroshima	B.j.jap. (Hiroshima)	AB159254	AB159470	AB159583
24. *Bufo japonicus japonicus*	Japan	Omogo, Ehime	B.j.jap. (Omogo)	AB159255	AB159471	AB159584
25. *Bufo japonicus japonicus*	Japan	Ono, Oita	B.j.jap. (Ono)	AB159256	AB159472	AB159585
26. *Bufo japonicus japonicus*	Japan	Kagoshima, Kagoshima	B.j.jap. (Kagoshima)	AB159257	AB159473	AB159586
27. *Bufo japonicus yakushimensis*	Japan	Yaku Isl, Kagoshima	B.j.yak.	AB159258	AB159474	AB159587
28. *Bufo japonicus miyakonis*	Japan	Miyako Isl, Okinawa	B.j.miy.	AB159259	AB159475	AB159588
29. *Bufo japonicus bankorensis*	Taiwan	Kuantzuling, Tainan	B.j.ban.	AB159260	AB159476	AB159589
30. *Bufo japonicus gargarizans*	China	Beijing	B.j.gar.	AB159261	AB159477	AB159590
31. *Bufo bufo*	Portugal	Minho	B.bufo	AB159262	AB159478	AB159591
32. *Bufo viridis* (outgroup)	Turkey		B.vir.	AB159263	AB159479	AB159592
33. *Bufo americanus* (outgroup)	USA	Ann Arbor, Michigan	B.ame.	AB159264	AB159480	AB159593

Table 2. Summary of alignment data and evolutionary models estimated with Modeltest (Posada and Crandall, 1998)

Alignment data	Total sites	Variable sites	Parsimoniously informative sites	Model
Cytochrome *b*	689	318	236	TrN+I+G
tRNAs	279	38	23	TrN+I
12S rRNA	411	57	28	TVM+I+G
16S rRNA	519	106	63	TrN+I+G
Combined data	2073	478	169	TrN+I+G

Table 3. Summary of phylogenetic analyses of the mitochondrial DNA gene fragments.

Node	Description	All combined data			Cytochrome *b*			tRNAs			12S rRNA			16S rRNA		
		ML	MP	NJ	ML	MP	NJ	ML	MP	NJ	ML	MP	NJ	ML	MP	NJ
1	*B. viridis* most basal	+(100)	+(100)	+(100)	+(93)	+(90)	+(99)	+(87)	+(87)	+(88)	+(68)	+(84)	+(89)	+(93)	+(99)	+(99)
2	*B. bufo* most basal in *B. bufo* species group	+(80)	+(100)	+(100)	+(58)	+(88)	+(90)	+(76)	+(88)	+(96)	+(60)	+(83)	+(90)	+	+(90)	+(91)
3	*B. j. gar. B. j. miy. B. j. ban.* most basal in *B. j. japonicus* group	+(65)	+(96)	+(99)	+	+(93)	+(99)	+	-	+(51)	-	-	-	+	-	+(91)
4	*B. j. torrenticola* in a clade with *B. j. japonicus* West Japan group	+(96)	+(98)	+(100)	+(95)	+(94)	+(100)	-	-	-	+(64)	+(54)	+(70)	+	-	+
5	*B. j. japonicus* East Japan group	+(99)	+(100)	+(100)	+(77)	+(98)	+(100)	+(62)	+(63)	+(67)	+(73)	+(73)	+(76)	-	-	+(82)
5a	*B. j. torrenticola* in a clade with *B. j. japonicus* East Japan group	-	-	-	-	-	-	-	-	+	-	-	-	-	-	-
5b	*B. j. gar. B. j. miy. B. j. ban.* in a clade with *B. j. japonicus* East japan group.	-	-	-	-	-	-	-	-	-	-	-	-	-	+	-
6	*B. j. japonicus* Kyusyu district sister to *B. j. torrenticola*	+(60)	+	-	-	-	-	-	-	-	+	+	+	-	-	+
6a	*B. j. japonicus* Chugoki Kinki Shikoku district sister to *B. j. torrenticola*	-	-	+	+	-	+(56)	-	-	-	-	-	-	-	-	-
6b	*B. j. torrenticola* most basal in *B. j. japonicus* West Japan	-	-	-	-	-	-	-	-	-	-	-	-	+	+	-
7	*B. j. japonicus* Kanto Tohoku Hokkaido district	+(94)	+(99)	+(100)	+(89)	+(84)	+(100)	+	-	+(55)	-	-	-	+(90)	+(92)	+(98)
8	*B. j. japonicus* Chubu Tokai Kanto district	+(97)	+(100)	+(100)	+(83)	+(96)	+(100)	-	+(57)	+	+(53)	-	+(54)	+(78)	+(82)	+(84)
9	*B. j. japonicus* Tohoku district	+(93)	+(96)	+(100)	+(99)	+(97)	+(99)	-	-	-	-	-	-	-	-	-
10	*B. j. japonicus* Kanto Hokkaido district	+(100)	+(100)	+(99)	+(100)	+(100)	+(100)	-	-	-	-	-	-	-	-	-
11	*B. j. miy. B. j. gar. B. j. ban.* in a clade	+(100)	+(100)	+(100)	+(100)	+(100)	+(100)	-	-	-	+(87)	+(86)	+(95)	+(73)	+(99)	+(100)
12	*B. j. jap.*(Hakodate) sister to *B. j. jap.*(Kashiwa)	+(95)	+(96)	+(93)	+(76)	+(82)	+(75)	-	-	-	+	-	+(59)	+	+(52)	+(63)
13	*B. j. jap.*(Zama) most basal in a *B. j. jap.* Kanto district	+(100)	+(98)	+(100)	+(91)	+(98)	+(98)	-	-	-	+(76)	+(84)	+(90)	+(73)	+(83)	+(86)
14	*B. j. miy.* sister to *B. j. gar.*	+(84)	+(90)	+(87)	+(79)	+(73)	+(87)	-	-	-	-	-	+	+(61)	+(62)	+(68)
15	*B. j. japonicus* Kinki Chugoku Shikoku district in a clade	+(100)	+(100)	+(100)	+(100)	+(100)	+(100)	+(79)	+(90)	-	+(83)	+(88)	+(88)	+(68)	+(92)	+(96)
16	*B. j. torrenticola* in a clade	+(100)	+(100)	+(100)	+(100)	+(100)	+(100)	-	-	-	+(88)	+(93)	+(97)	+(99)	+(99)	+(100)
17	*B. j. japonicus* Kyushu district in a clade	+(100)	+(100)	+(100)	+(100)	+(100)	+(100)	+(61)	+(71)	-	+(87)	+(91)	+(98)	+(62)	+(90)	+(99)

+, a certain topology was supported in analysis; -, the topology was not supported. Numbers in parentheses are bootstrap support values (ML, MP, and NJ) (only given if >50%)

Note. Combined and separate ML analyses recovered single topology with highest –logML (shown in Table 4). The –logML were 7707.14526, 5081.08200, 650.15971, 1029.49256, and 1641.63165, for combined data, Cyt *b*, tRNAs, 12S rRNA, and 16S rRNA, respectively. As for MP analyses, combined data reconstructed 110 maximum parsimonious trees (length = 1,360, CI = 0.6593, and RI = 0.8218). Separate data made following MP trees: Cyt *b*, the consensus tree of twelve trees (length = 664 steps CI = 0.6057 RI = 0.8067); tRNAs, the consensus tree of fifty two trees (length = 57 steps CI = 0.7018 RI = 0.8317); 12S, the consensus tree of eighty trees (length = 84 steps CI = 0.7976 RI = 0.8859); 16S, the consensus tree of 179 trees (length = 187 steps CI = 0.6684 RI = 0.8019).

Table 4. Complete mitochondrial genomes used in this study

Taxon	Species	Accession nos.
Order Anura		
"Archaeobatrachia"*		
Bombinatoridae	*Bombina bombina*	AY458591
	Bombina orientalis	AY585338
Discoglossidae	*Alytes obstetricans pertinax*	AY585337
	Discoglossus galganoi	AY585339
Pipidae	*Xenopus laevis*	M10217
	Xenopus tropicalis	AY789013
Suborder Neobatrachia		
Superfamily Hyloidea		
Bufonidae	*Bufo melanostictus*	AY458592
Hylidae	*Hyla chinensis*	AY458593
Superfamily Ranoidea		
Microhylidae	*Microhyla heymonsi*	AY458596
	Kaloula pulchra	AY458595
Mantellidae	*Mantella medagascariensis*	AB212225
Rhacophoridae	*Rhacophorus schlegelii*	AB202078
	Buergeria buergeri	AB127977
Ranidae	*Fejervarya limnocharis*	AY158705
	Rana nigromaculata	AB043889
Urodela		
Cryptobranchidae	*Andrias davidianus*	AJ492192
Salamandridae	*Lyciasalamandra atifi*	AF154053
Salamandridae	*Paramesotrition hongkongensis*	AY458597
Hynobiidae	*Ranodon sibiricus*	AJ419960
Gymnophiona		
Ichthyophiidae	*Ichthyophis bannanicus*	AY458594
Rhinatrematidae	*Rhinatrema bivittatum*	AY456252
Caeciliidae	*Typhlonectes natans*	AF154051
Amniota		
Crocodylidae	*Alligator mississippiensis*	Y13113
Bovidae	*Bos Taurus*	J01394
Phasianidae	*Gallus gallus*	X52392
Hominidae	*Homo sapiens*	AF347015
Dipnoi		
Protopteridae	*Protopterus dolloi*	L42813
Actinopterygii		
Scyliorhinidae	*Scyliorhinus canicula*	Y16067
Cyprinidae	*Cyprinus carpio*	X61010

*Generally, "Archaeobatrachia" is regarded as a paraphyletic group with respect to Neobatrachia.

Tabke 5. Reference points used in this strudy and recent studies

Node	Time constraint (Mya)			Reference	Reference point setting (ref-set)		
	This study	San Mauro et al., (2005)	Zhang et al., (2005)		1	2	3
Dipnoi – Tetrapoda	410 – 390*		410 – 390*	Benton, (1990)	○	○	○
diapsids - synapsids	320 – 300		320 - 300	Kumar and Hedges, (1998)	○	○	
crocodile – bird	252 – 257	> 161		Reisz and Müller, (2004a)	○	○	○
Hynobiidae - Cryptobranchidae	167 – 157			Gao and Shubin, (2001)	○	○	○
Rhacophoridae – Mantellidae	92.6 – 53.6	> 230		Bossuyt and Milinkovitch, (2001)	○		○
Anura – Urodera	> 230	> 140		earliest fossil record of Salientina *Triadobatrachus*; Rage and Rocek, (1989)	○	○	○
Pipids – other sister groups	> 135			earliest fossil record of Pipids frog; Rocek (2000)	○	○	○
Discoglossidae – Bombinatoridae	> 168	> 53		earliest fossil record of Discoglossids frog; Milner (1993)	○	○	○
Caudiverbera and *Lechriodus*		> 86		Fossil record of *Caudiverbera*; Baez (2000)			
South American pipids - African pipids		> 86		Separation of Africa and South America; Pitman et al. (1993)			
Agalychnis - Litoria		> 42		Last connection between Australia and South America; Seddon et al. (1998)			
Mantidactylus wittei – Mantidactylus sp.		< 15		Volcanic origin of the oldest Comoro island myotte; Vences et al. (2003)			

* These value were used as a prior assumption of ingroup node (rttm) and a standard deviation (rttmsd) in multidivtime program.

Table 6. Compositional features of mt genomes

Feature	*Bufo japonicus*		*Hyla japonica*		*Microhyla okinavensis*	
Total length	17,757		19,519		16,717	
% A	28.9		29.6		29.0	
% C	27.6		25.4		24.6	
% G	15.3		14.5		14.5	
% T	28.1		30.5		31.8	
control region	2,351		4,103		1,335	
12S rRNA	930		933		934	
16S rRNA	1,600		1,600		1,581	
ATPase6	684	(ATG/TAA)	683	(ATG/TA-)	682	(ATG/T--)
ATPase8	165	(ATG/TAA)	165	(ATG/TAA)	165	(ATG/TAA)
CO1	1,542	(ATA/TAA)	1,542	(ATA/AGG)	1,551	(ATA/AGG)
CO2	688	(ATG/T--)	688	(ATG/T--)	688	(ATG/T--)
CO3	779	(ATG/AGG)	758	(ATG/TA-)	784	(ATG/T--)
Cytb	1,146	(ATG/AGA)	1,149	(ATG/TAG)	1,143	(ATG/TAA)
ND1	961	(TTG/T--)	961	(TTG/T--)	958	(GTG/T--)
ND2	1,035	(ATC/TAG)	1,035	(ATT/AGA)	1,033	(ATG/T--)
ND3	340	(ATG/T--)	340	(ATG/T--)	340	(ATG/T--)
ND4	1,365	(ATG/TAA)	1,365	(ATG/TAA)	1,363	(ATG/T--)
ND4L	300	(ATG/TAA)	303	(ATG/TAA)	285	(ATG/TAA)
ND5	1,803	(ATG/AGA)	1,803	(ATG/AGA)	1,806	(ATG/AGG)
ND6	495	(ATG/AGA)	495	(ATG/AGA)	498	(ATG/TA-)

Parentheses show the start and stop codons. ('-' means incomplete termination of stop codons).

Table 7. Summary of branch support values

Dataset		a	b	c	d	e	f	g	h	i	j	k	l	m	n	o	p	q	r	s	t	u	v	w	x	y
Proteins (Amino acids)	**ML**	100	88	69	85	100	100	100	66	80	99	100	100	100	100	100	100	98	69	100	100	100	100	95	100	86
	BPP	100	100	100	100	100	100	100	99	100	100	100	100	100	100	100	100	100	100	99	100	100	100	100	100	100
	MP	97	-	-	-	100	100	99	-	-	88	100	100	100	100	100	99	76	100	55	100	100	81	100	100	-
Proteins + rRNAs	**ML**	100	98	58	100	100	100	100	65	99	100	100	100	100	100	100	100	100	98	100	100	100	100	100	100	96
(Nucleotides)	**BPP**	100	100	53	100	100	100	100	100	100	100	100	100	100	100	100	100	100	100	100	100	100	100	100	100	100
	MP	86	79	66	66	100	100	100	-	-	78	100	100	100	100	100	86	91	100	85	100	100	100	100	100	-

Proteins (Amino acids): the concatenated amino acid data of 12 protein genes. Proteins+ rRNAs (Nucleotides): the concatenated nucleotide sequece data of 12 protein and two rRNA genes. a - x show the nodes in Fig. 7.

Table 8. Comparison of divergence times of branching node in Lissamphibia with their standard deviation (SD) and 95% confidence intervals (CI) estimated in this study and previous studies

Branching node	Branching time (Ma)	SD	95% CI (Ma)	Reference
Gimnophiona – other Lissampbhia (C)	335	9	317-351	Present study
	337	–	321-353	Zhang et al. (2005a)
	367	23	328-417	San Mauro et al. (2005)
Urodera – Anura (D)	318	9	298-337	Present study
	308	–	289-328	Zhang et al. (2005a)
	357	22	317-405	San Mauro et al. (2005)
Archaeobatrachia – Neobatrachia (E)	297	12	274-319	Present study
	290	–	268-313	Zhang et al. (2005a)
	262 *	21	223-305	San Mauro et al. (2005)
Ranoidea – Hyloidea (F)	170	16	140-202	Present study
	173	–	152-195	Zhang et al. (2005a)
	150	18	117-186	San Mauro et al. (2005)
	Approx. 170	–	–	Vences et al. (2003)
Raniodae – Microhylidae (G)	122	15	95-151	Present study
	142	–	123-162	Zhang et al. (2005a)
	99	16	70-132	San Mauro et al. (2005)
	134	20	99-177	van der Meijden (2005)
Bufonidae – Hylidae (K)	97	18	65-133	Present study
	97	–	81-115	Zhang et al. (2005a)
	65	8	52-84	San Mauro et al. (2005)
***Micohyla – Kaloula* (L)**	81	13	58-107	Present study
	96	–	81-113	Zhang et al. (2005a)

C – G, K, and L correspond to the nodes in Fig. 9. Present study refers to the estimated divergence times based on amino acid data in this study (Fig. 9). San Mauro et al. (2005) refers to their estimated divergence times mentioned as 'multiple calibration'. *This value means the split of neobatrachians from archaeobatrachians, because San Mauro et al. (2005) suggested the paraphyly of archaeobatrachians with respect to neobatrachians.

Table 9. Comparison of divergence times based on three datasets with three distinct reference point settings

	(1) Proteins (Amino acids)			(2) Proteins + rRNAs (Nucleotides)			(3) Proteins+ rRNAs (Nucleotides –3rd)		
Branching node	ref-set 1	ref-set 2	ref-set 3	ref-set 1	ref-set 2	ref-set 3	ref-set 1	ref-set 2	ref-set 3
Dipnoi/Rhipidistia – Tetrapoda (A)	393 (407 – 378)	393 (407 – 378)	395 (408 – 379)	391 (405 – 376)	392 (405 – 376)	395 (408 – 380)	391 (406 – 375)	391 (406 – 375)	395 (408 – 379)
Amniota – Amphibia (B)	355 (370 –340)	355 (369 – 340)	358 (376 – 340)	358 (369 – 345)	358 (371 – 346)	364 (379 – 349)	358 (372 – 344)	358 (372 – 343)	365 (381 – 348)
Gymnophiona - Caudata/Anura (C)	335 (352 – 298)	335 (352 – 317)	338 (358 – 318)	334 (348 – 320)	336 (350 –322)	341 (357 – 324)	335 (351 – 319)	336 (352 – 319)	343 (361 – 323)
Urodela – Anura (D)	318 (337 – 298)	318 (337 – 297)	321 (342 – 299)	322 (336 – 307)	323 (338 – 308)	328 (345 – 311)	321 (338 – 303)	321 (338 – 203)	328 (347 – 307)
Neobatrachia – Archiobatrachia (E)	297 (319 – 274)	297 (319 – 272)	300 (324 – 274)	292 (308 – 274)	296 (313 –277)	298 (317– 278)	294 (313 – 271)	294 (315 – 272)	300 (323 – 276)
Ranoidea – Hyloidea (F)	170 (202 – 140)	171 (209 – 133)	171 (203 – 140)	171 (190 – 150)	183 (209 – 156)	174 (193 – 153)	170 (198 – 141)	173 (207 – 139)	174 (202 – 143)
Microhylidae – Ranidae (G)	122 (150 – 95)	123 (164 – 86)	122 (152 – 95)	127 (142 – 108)	140 (167 – 114)	128 (143 – 110)	123 (149 – 97)	127 (162 – 94)	126 (151 – 98)
Mantellidae – Rhacopholidae (J)	73 (91 – 55)	74 (104 – 48)	73 (91 – 55)	85 (92 – 72)	97 (119 – 76)	86 (92 – 73)	75 (91 – 57)	78 (105 – 55)	76 (91 – 57)
F.limonocaris - other ranoids (H)	93 (117 – 71)	94 (131 - 63)	94 (117 - 72)	107 (119 – 90)	120 (145– 96)	108 (120 – 92)	99 (119 – 76)	102 (134 – 72)	100 (21 – 77)
Bufonidae – Hylidae (K)	97 (133 – 65)	97 (143 – 60)	97 (133 – 65)	111 (131 – 91)	123 (151 – 96)	113 (132 – 92)	101 (132 – 72)	104 (142 – 71)	103 (133 – 73)

Values in parenthesis show 95% confidence intervals. A – G, H, J, and K correspond to the nodes in Fig. 9. Ref-sets 1-3 mean reference point settings.

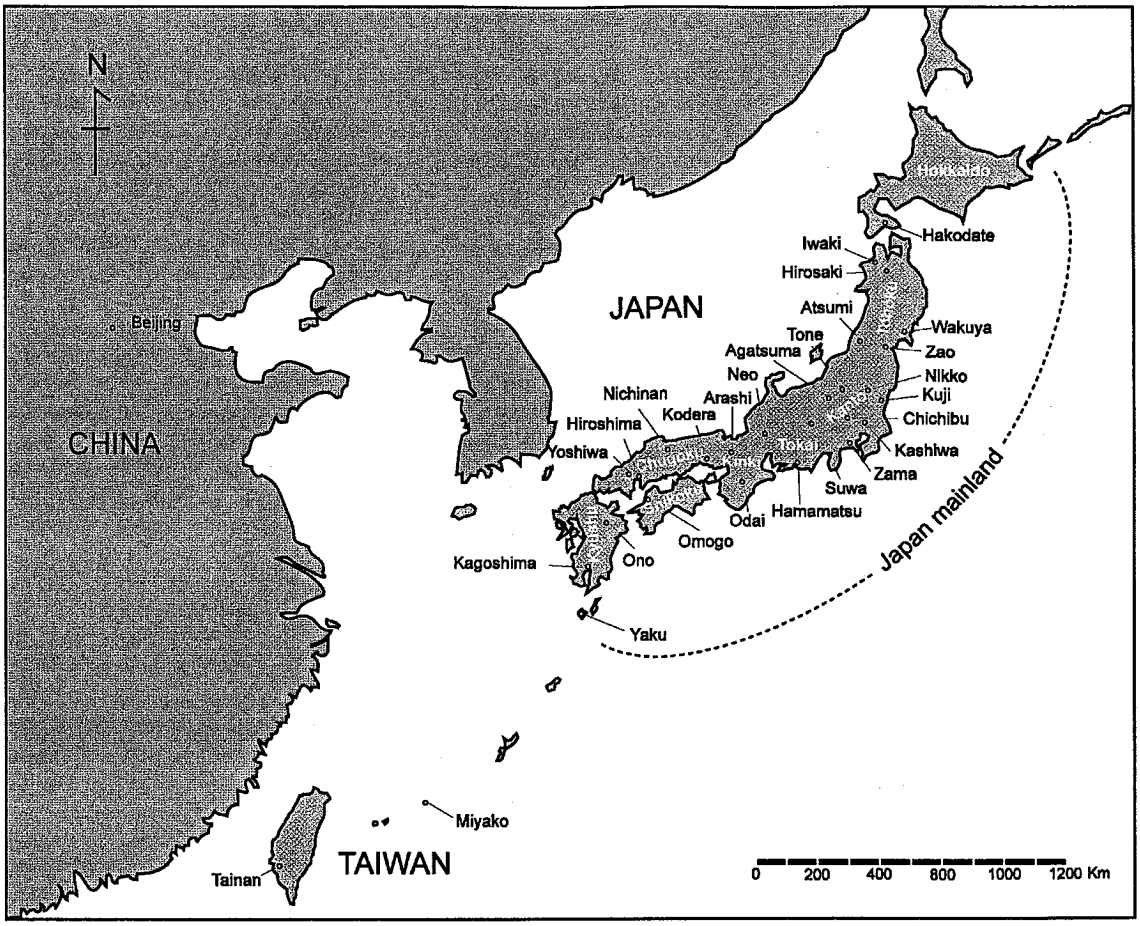

Fig. 1. Map showing the collecting stations of the toads used in the present study.

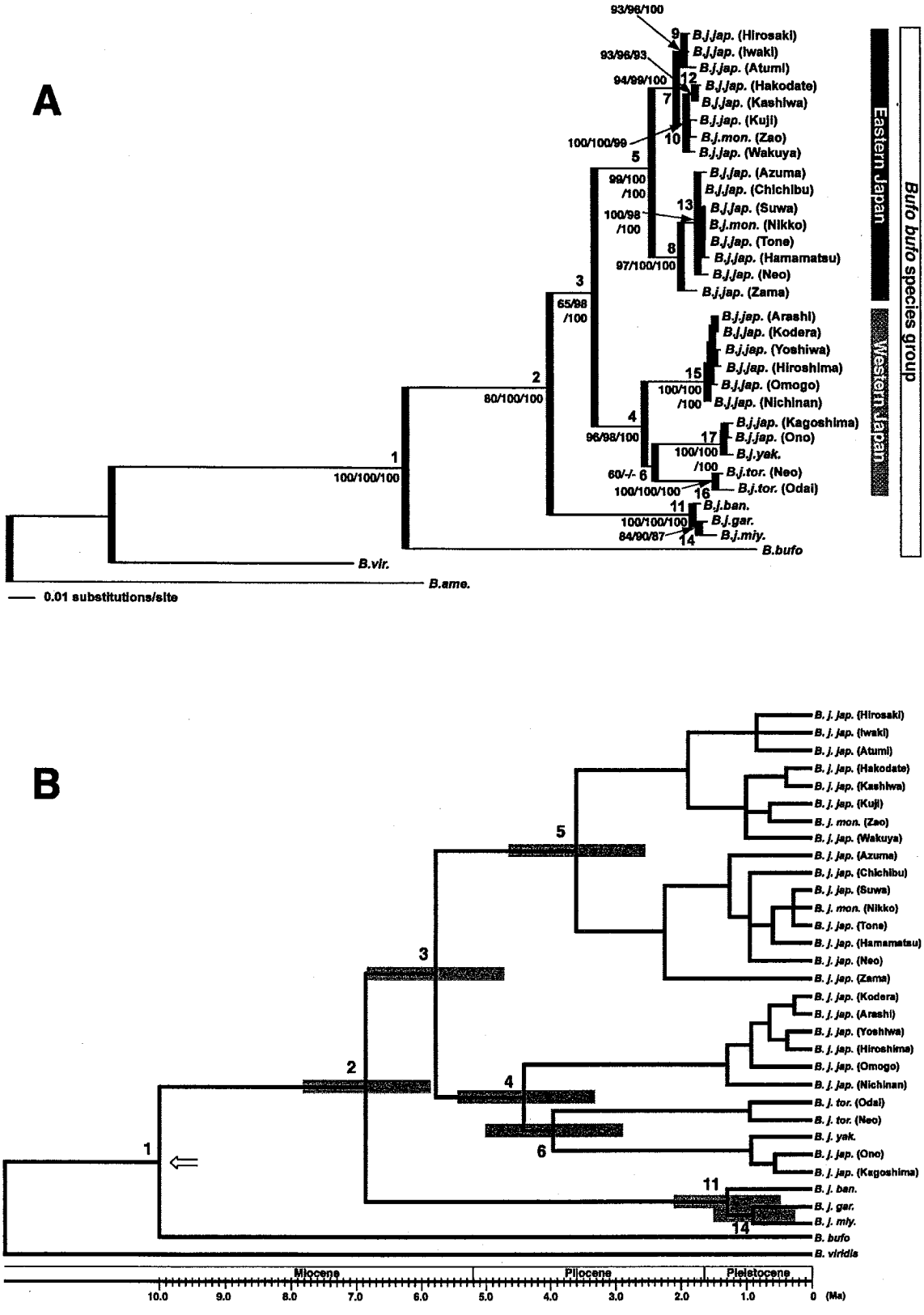

Fig. 2. (A) Maximum Likelihood tree (-ln *L*= 7707.14526) of 33 *Bufo* taxa obtained based on 2,075bp of the mitochondrial DNA genes with the TrN+I+G substitution model. The numbers of each clade correspond to those in the text and Table 4. The Bootstrap supports are given in order for ML/MP/NJ. (B) ML tree topology of the combined dataset converted to an ultrametric tree by estimating the relative divergence dates of the *Bufo* species used in this study. As a fixed reference point, we used the split between European and Asian *Bufo* species (*B. bufo* and the *B. japonicus* subspecies group) (indicated by an arrow).

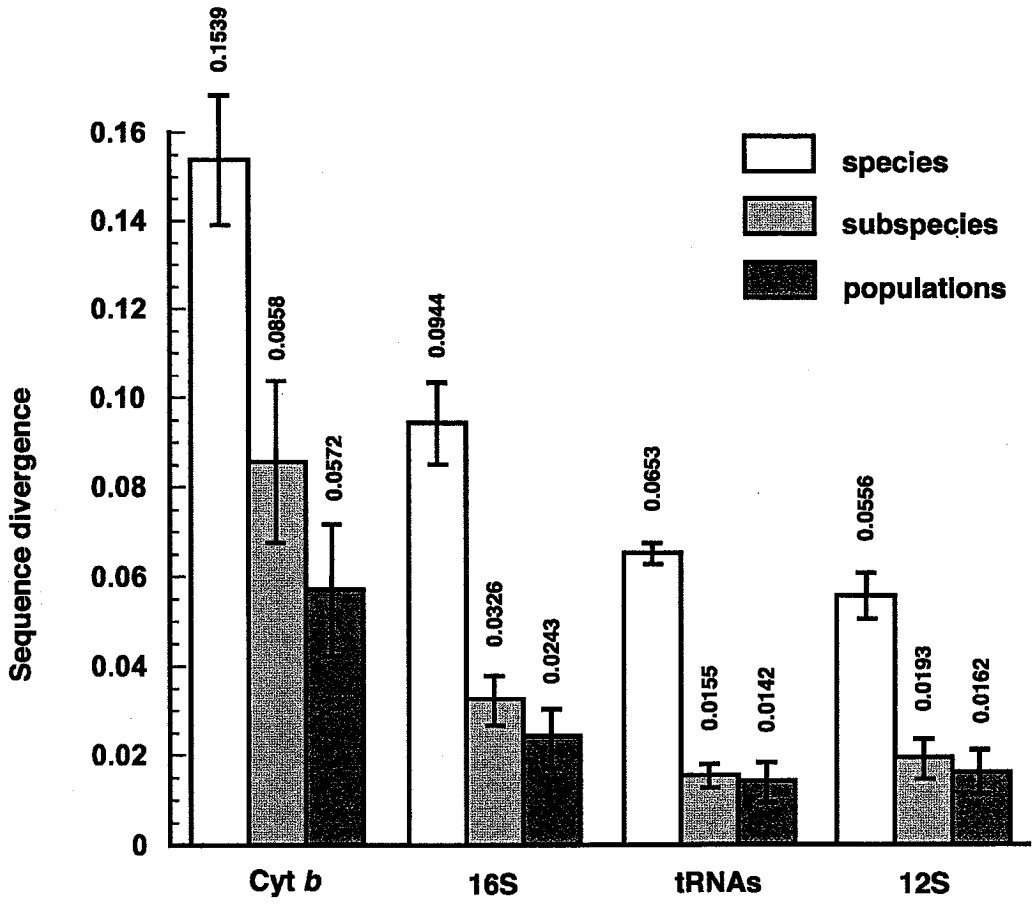

Fig. 3. Comparisons of the average sequence divergences of the mitochondrial DNA genes among three different taxonomic levels.

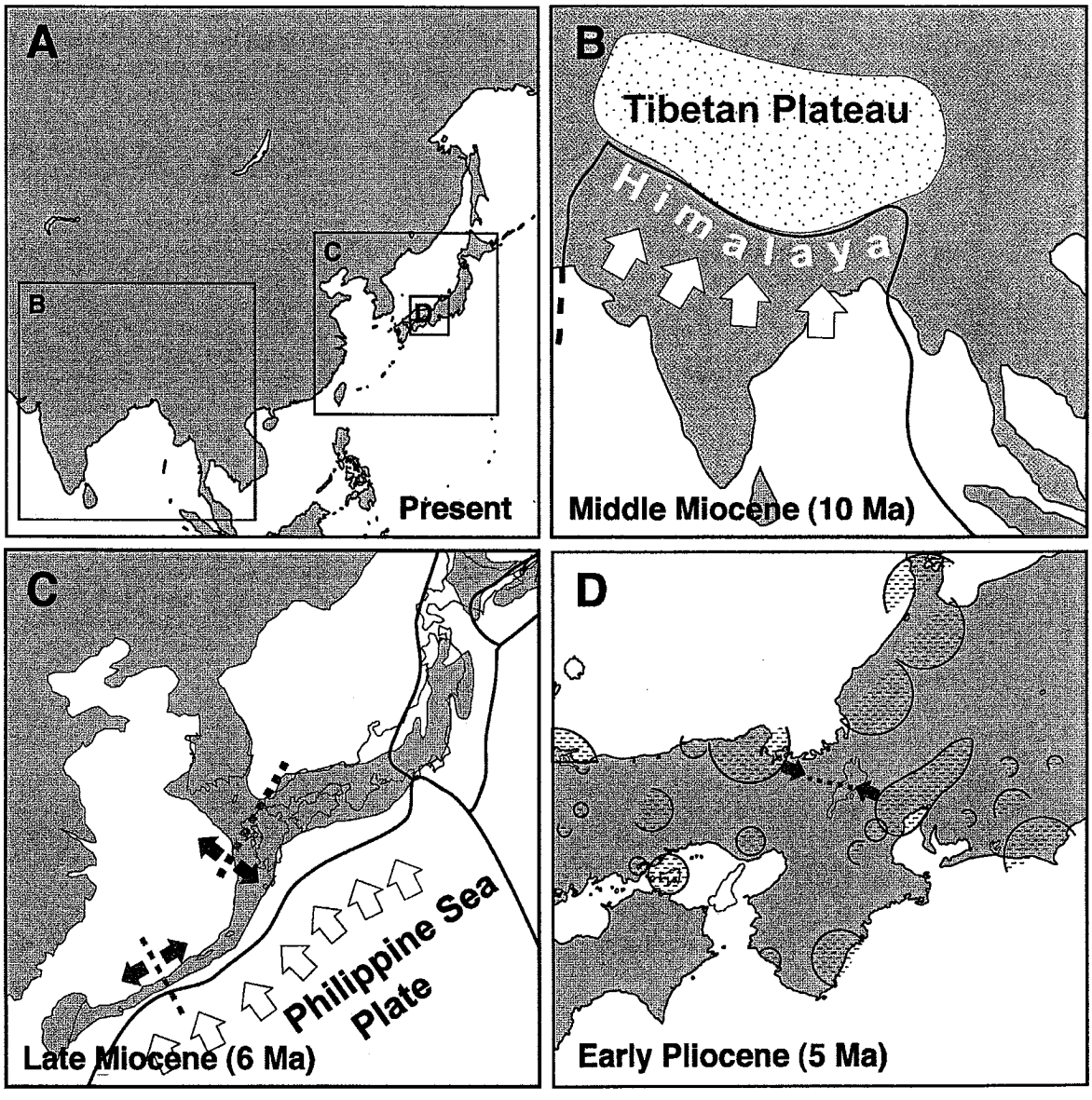

Fig. 4. Summary of the paleogeography in eastern Asia. (A) Map of Eastern Asia at present showing areas represented in the other paleogeographic maps. (B) Paleogeographic map of Southern Asia (Middle Miocene, 10 Ma; modified from Harrison et al., 1992). The solid line indicates the Indian Plate and open arrows indicate movements of the Indian Plate and Indian subcontinent. (C) Paleogeographic map of Eastern Eurasia and the Japanese Archipelago (Late Miocene, 6 Ma; modified from Maruyama et al., 1997 and Kamata and Kodama, 1999). The solid line indicates plates in this area and open arrows indicate movements of the Philippine Sea Plate. Dotted lines and solid arrows indicate the area where land dividing events are expected. (D) Paleogeographic map of the central Japan mainland (Early Pliocene, 5 Ma; modified from Itoigawa, 1991 and Yoshida 1992). Dotted circles indicate the ancient basin. The dotted line and solid arrows indicate the direction of basin expansion.

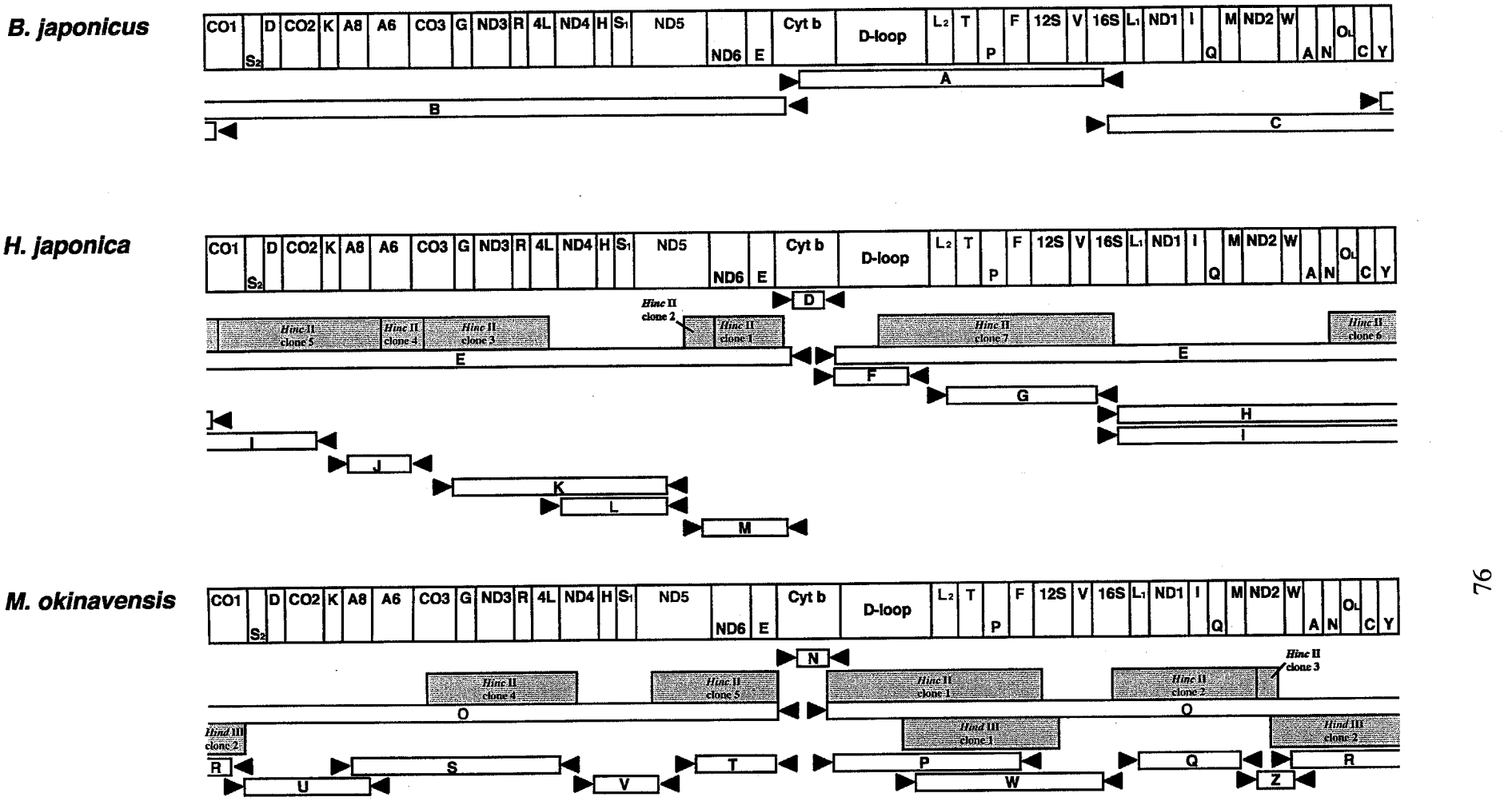

Fig. 5. PCR-amplification strategies of *B. japonicus, H. japonica,* and *M. okinavensis* mtDNAs and gene maps shown by linear representations. *H*- and *L*-strand-encoded genes are denoted above and below each map, respectively. Transfer-RNA genes are designated by single-letter amino acid codes. L1, L2, S1, and S2 indicate tRNA genes for Leu(UUR), Leu(CUN), Ser(UCN), and Ser(AGY), respectively. Other genes are abbreviated as followings: 12S and 16S, 12S and 16S ribosomal RNA genes; A6 and A8, ATPase subunits 6 and 8 genes; CO1-3, cytochrome oxidase subunits I-III; Cytb, cytochrome *b*; ND1-6 and 4L, NADH dehydrogenase subunits 1-6 and 4L. CR1 and CR2 indicate control regions 1 and 2, respectively. O_L denotes putative *L*-strand replication origins. Open boxes under each gene map show the amplified PCR fragments, and closed arrows indicate the locations and directions of the amplification primers. Shaded boxes specify the cloned fragments.

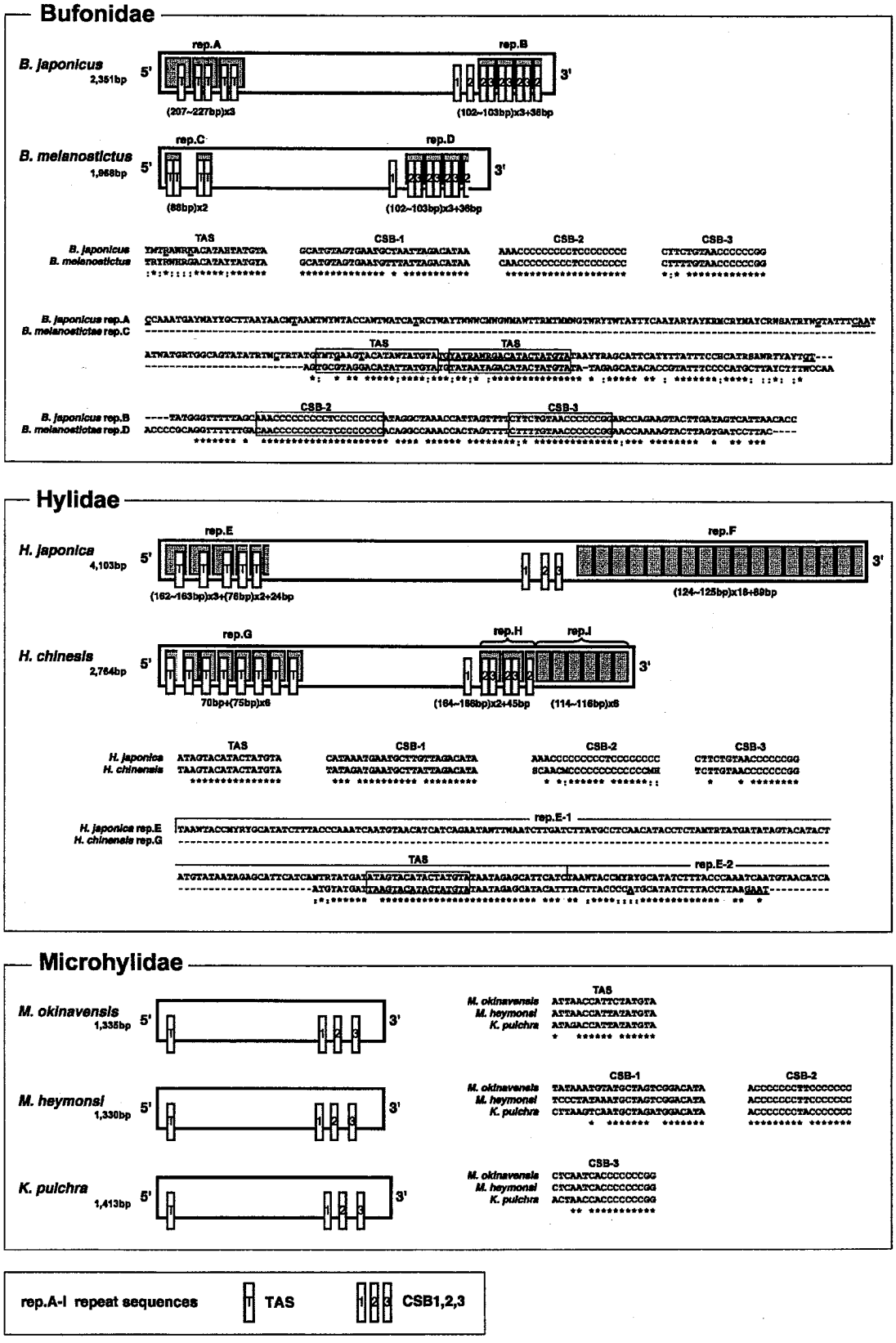

Fig. 6. Comparisons of the control region structures and alignments of characteristic sequences. For each family, structures of control region and alignments of identified putative termination-associated sequences (TAS), conserved sequence blocks (CSB 1 - 3), and repeat motifs are shown. In the alignments, H, K, S, W, M, Y, and R show alternative nucleotides between repeat units (H = A / T /G, K = G / T, S = G / C, W = A / T, M = A/ C, Y = C / T, R= A / G). Underlined nucleotides indicate deleted nucleotides in some units.

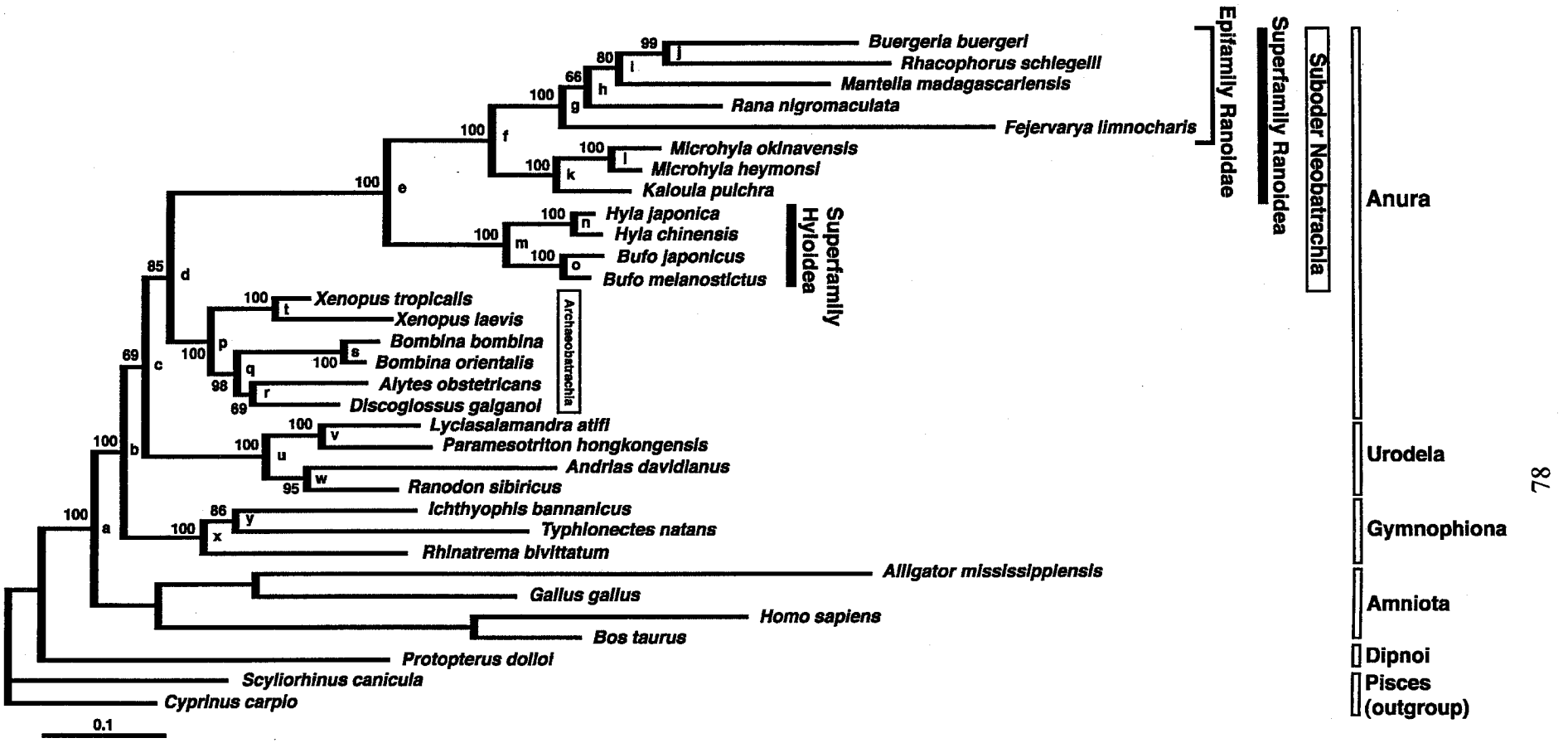

Fig. 7. Maximum-likelihood (ML) tree (–ln*L* = –67443.20) based on the 3,197 concatenated amino acid sites with the mtREV + Γ model. The horizontal length of each branch corresponds to the substitution rates estimated with the model. Two ray-finned fishes (*Scyliorhinus canicula* and *Cyprinus carpio*) were used as outgroups. Numbers on braches are percent nonparametric bootstrap probability (nBP).

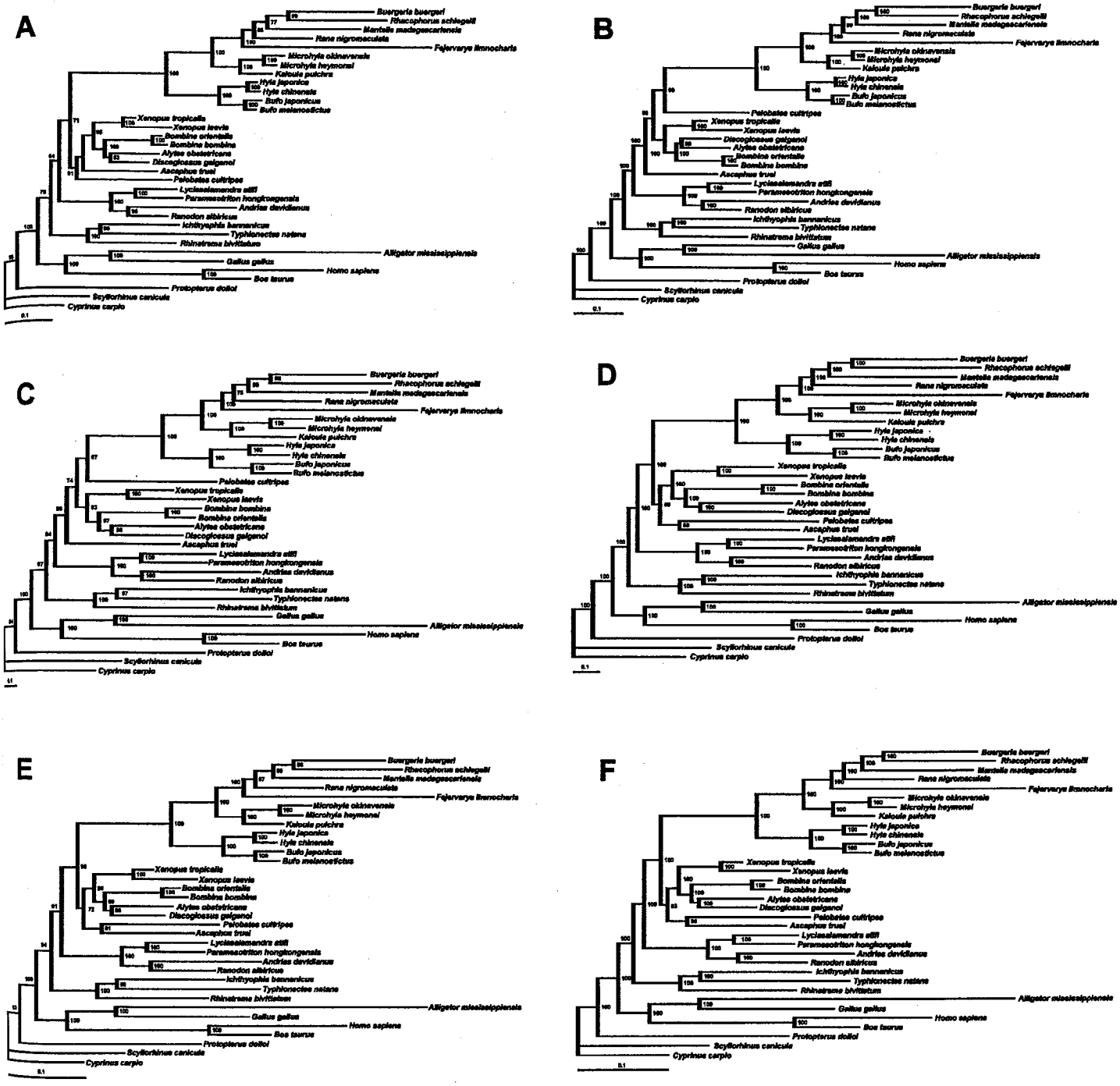

Fig. 8. (A) Maximum-likelihood (ML) tree (-ln*L* = -70654.71) and (B) Bayesian tree based on the 3,196 concatenated amino acid sites of 12 protein genes with the mtREV + Γ model. (C) ML tree (-ln*L* = -219096.68) and (D) Baysian tree based on the 11,029 concatenated nucleotide sites of all codon site of 12 protein genes and two rRNA genes with the GTR + Γ + I model. (E) ML tree (-ln*L* = -99263.74) and (F) Bayesian tree based on the 7,833 concatenated nucleotide sites of 1st and 2nd codon sites of 12 protein genes and two rRNA genes with the GTR + Γ + I model. Numbers on branches are percent nonparametric bootstrap probability or Bayesian posterior probailities.

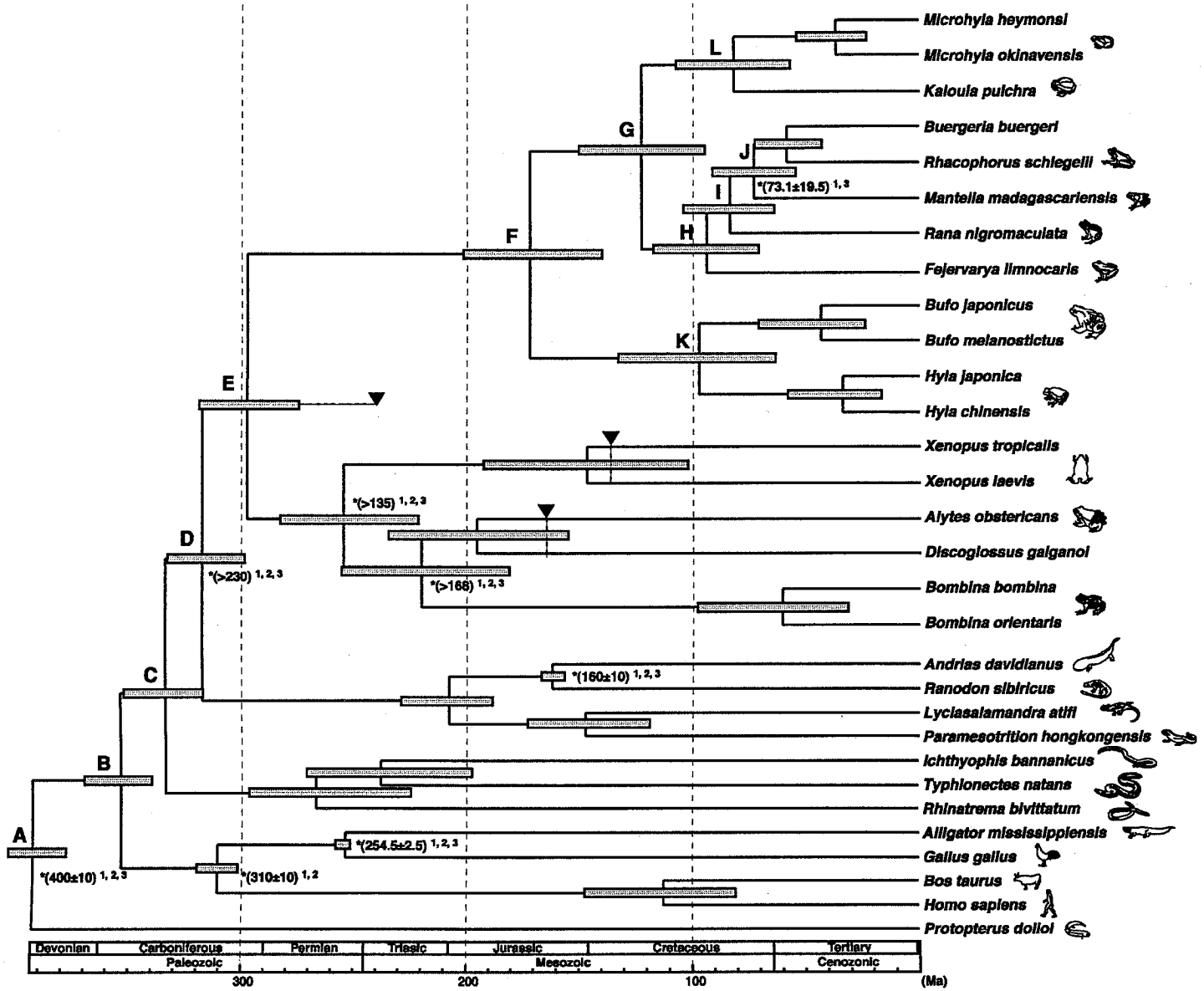

Fig. 9. Estimated divergence times and their 95% credibility intervals (hatched rectangles) inferred from the amino acid sequence of 12 protein genes. Phylogenetic relationships were assumed based on results of Fig. 7. The Multidivtime software package (Thorne et al., 2002) was used with seven reference points indicated by asterisks. Superior numbers at reference points show 3 different settings (ref-sets 1 – 3) (see Table 5). Filled triangles show ages of oldest fossils records of corresponding taxa.

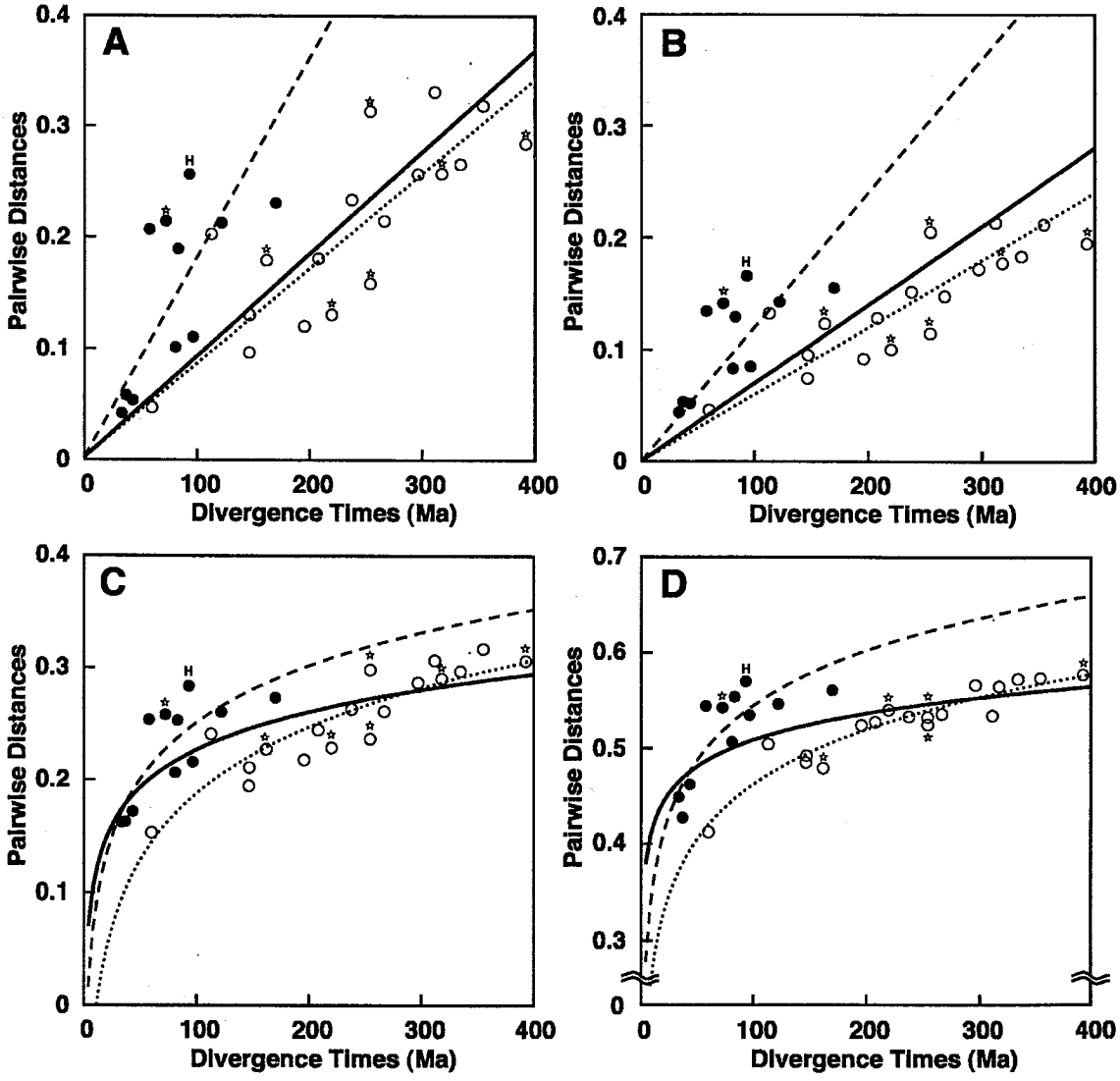

Fig. 10. Plots of pairwise distances calculated from (A) concatenated amino acid data of 12 protein genes, (B) concatenated nucleotide data of 1st and 2nd codon sites of 12 protein genes and two rRNA genes, (C) concatenated nucleotide data of all codon sites of 12 protein genes and two rRNA genes, and (D) concatenated nucleotide data of 3rd codon sites of 12 protein genes. The divergence time used here are based on amino acid sequences of 12 protein genes (dataset 1) with all 7 reference points (ref-set 1). Pairwise distances were calculated using PAUP* (Swofford, 2001) and plotted by averaging values for all corresponding species pairs. Circles express pairwise distances among non-neobatrachians, and solid circles show those among neobatrachians. Solid, broken and dotted lines (and/or curves) are regressions of pairwise distances vs branching times between all taxa, between neobatrachians, and between non-neobatrachian species, respectively. Open stars indicate the branchings that were used as reference points. 'H' indicates pairwise distance between *F. limnocalis* and the other ranoids.

公表論文

(1) Molecular phylogenetic relationship of toads distributed in the Far East and Europe inferred from the nucleotide sequences of mitochondrial DNA genes.
Takeshi Igawa, Atsushi Kurabayashi, Midori Nishioka, M. Sumida
Molecular Phylogenetics and Evolution, 38 (2006) 250 – 260

(2) Complete mitochondrial genomes of three neobatrachian anurans: A case study of divergence time estimation using different data and calibration settings.
Takeshi Igawa, Atsushi Kurabayashi, Chisako Usuki, Tamotsu Fujii, Masayuki Sumida
Gene, 407 (2008) 116 – 129